International Journal of Dynamics and Control (2024) 12:1366–1391
https://doi.org/10.1007/s40435-023-01284-5

Dynamics of spatio-temporal HIV–AIDS model with the treatments of HAART and immunotherapy

Mohammad Ghani[1]

Received: 22 February 2023 / Revised: 19 July 2023 / Accepted: 8 August 2023 / Published online: 22 August 2023

Abstract
In this paper, we focus on the study of HIV–AIDS model in space and time that is adapted from the previous study in Ammi et al. (Sci Rep 12:5751, 2022) without the fractional-order derivative. The fixed controls of highly antiretroviral and immunotherapy are considered for the interaction between susceptible and infected $CD4^+T$ cell. The equilibrium points of disease-free and endemic, positivity, boundedness and basic reproduction number of dynamical system are provided in the standard ways. For the local stability, the Fourier series is firstly employed to obtain the Jacobian matrix which is then used for further analysis of stability. Moreover, the classical numerical scheme of standard finite difference is applied to approximate our model. The stability, positivity, and consistency of numerical scheme are very important in the numerical analysis. At the last section of numerical analysis, we provide the experiments of our model numerically by varying values for the parameters of treatment HAART and Immunotherapy. We can conclude that the combinations of HAART and Immunotherapy at once are the most efficient in decreasing the infected $CD4^+T$ cells and the treatment of immunotherapy is more effective than the treatment of HAART. Our dynamical system is eligible to predict the spread of HIV–AIDS based on the validation results with the actual data by using least square technique. Moreover, we apply the ARIMA(1,1,0) model in this paper to predict infected profile and the result has the similar trend (decreasing trend) with the HIV–AIDS model (obtained from the least square technique) and the actual data. Moreover, we employ the neural network for dynamical system, due to the significant results of best validation performance, error histogram, and regression.

Keywords HIV–AIDS model · Standard finite difference · Highly active antiretroviral therapy · Immunotherapy · Basic reproduction number · Least square technique · Disease transmissions · Neural network

Mathematics Subject Classification 35A01 · 35B40

1 Introduction

Human Immunodeficiency Virus (HIV) infectious disease presents a significant obstacle to public health professionals in both developing and developed countries [1–3]. According to the United Nations for AIDS (UNAIDS) reports, 37.9 million people worldwide had HIV as of the end of 2018, and approximately one million people died each year because of infection's symptoms of HIV. In 2030, UNAIDS makes some plan to eliminate the disease. The retrovirus HIV can attack the immune's system of human CD4 cells [4, 5]. Moreover, HIV keeps attacking further CD4 cells continuously if the infected individuals are left untreated. The worst thing, the HIV infection will be in the most critical level, i.e., in stage of Acquired Immunodeficiency Syndrome (AIDS). In general, AIDS takes about 2–10 years to reach its maximal stage [6]. During that stage, the ability of immune's system is much too insufficient to counter infectious diseases such as tuberculosis [7, 8], cryptococcal meningitis [9, 10], cryptosporidiosis [11], as well as cancers. In general, HIV is transmitted through bad behavior of sexual, and blood's transfusion. The infection's symptoms of HIV involve muscle aches, swollen lymph nodes, fever, and weight loss. Most infected individuals of HIV do not show the obvious infection's symptoms. Because the infection's symptoms are possibility associated with other indications, laboratory testing is the appropriate manner to monitor the HIV stage. Around 8.1 million of

✉ Mohammad Ghani
mohammad.ghani2013@gmail.com

[1] Faculty of Advanced Technology and Multidiscipline, Universitas Airlangga, Surabaya 60115, Indonesia

infected individuals are generally unaware of their HIV status. People are discouraged from testing for HIV because of factors such as social stigma, discrimination, and the high cost of health care [12]. HIV-1 and HIV-2 are two distinct strains of the virus. Moreover, several more genetically different subgroups of HIV exist in HIV-1 and HIV-2. Besides that, HIV-1 was more infective than HIV-2, which is primarily discovered in West Africa. At the present moment, there is no vaccine to eliminate the virus because of the HIV's ability to mutate. Moreover, AntiRetroviral Therapy (ART) has ability to reduce the infected individuals and prevent the disease from spreading. The life expectancy of HIV patients totally depends on the level of infection. The average survival rate for an HIV-infected individual without treatment is between 9 and 11 years, but appropriate treatment with ART can increase the patient's average lifespan to more than 10 years after the onset of AIDS [6]. Moreover, the UNAIDS has a plan to eliminate AIDS from the planet in the last year 2030. In the last year 2020, 90% of HIV infected individuals will be aware of HIV status. Government officials are requiring intersectoral and organized actions to eliminate HIV infection from the country, such as unrestricted access to HIV laboratory equipment, the ART's accessibility for infected individuals of HIV, and full adherence to testing prior to transfusion of blood and the utilization for disinfected equipment in health facilities and barbers. It is critical to raise the general public's level of awareness.

Many infectious diseases are transmitted through unrestricted population interaction. The medical staff recommends isolation or quarantine for the infected person. Many infectious disease models do not account for this critical factor. Because of this, simple mathematical models were unsuitable for disease dynamic behavior. We further adapted the dynamical system by adding the diffusion terms and two treatments of HAART and Immunotherapy in the continuous system to account for this omitted aspect in a simple system of differential equations HIV–AIDS. Moreover, the case of dynamical system HIV-1 under the delay factor was studied in [13], where this model is further studied as in [14]. Other studies of HIV–AIDS model under the delay factor can be found in [15–21]. The media can play a significant role for understanding in population referring to HIV/AIDS infectious disease in this digital era, by encouraging the individuals to take precautions through regards to infectious disease. As a consequence, social media sites are powerful and efficient equipment that can be utilized to inform the public regarding preventing infection as well as contagious diseases including HIV/AIDS [22]. Complex dynamical behaviors of a simple unified SIR and HIV disease model were addressed in [23]. Moreover, the SIR epidemic model with various basic reproduction numbers was studied in [24]. Based on the HIV and TSWV data, the SIR epidemic model was verified. The analytical solution provides an accurate approximation of both the experimental and clinical data. As a consequence, they can make the argument that their proposed solution is helpful for exhibiting the influence of epidemics and the fundamental factual information controlling the transmission of infectious diseases. Moreover, the transmission of infectious diseases can be more actually prevented and monitored with approaches that rely on their proposed solution. A nonlinear fractional order epidemic model was proposed and evaluated in [25] for HIV transmission with extended compartment particularly regarding exposed class to the basic SIR epidemic model. They as well established a fractional optimal control problem condition for such proposed model. It was used to solve the fractional optimal control problem related to control techniques including such contraceptive use in the exposed class, treatment for aware infectives, disease awareness between some of unaware infectives, and behavioral change for susceptible. The result revealed that control measures significantly enhance the age limit and life quality of HIV patients while somehow significantly decreasing the number of HIV/AIDS patients throughout epidemic. Through with a mathematical model, efforts made to prevent and treat HIV/AIDS may also be analyzed. For instance, the global asymptotical stability of new fractional order HIV/AIDS models was evaluated in [26] with treatment compartment and switching parameters, and the results showed that if the threshold value is lower than one, the disease can potentially be released; the impact of trying to rehabilitate treatments on the control of HIV/AIDS spread in prisons was examined in [27], as well as the results indicated that the use of treatment methods for drug abuse removal can decrease HIV/AIDS transmission. Another of the HIV/AIDS drug treatments, HAART (highly active antiretroviral therapy), commonly keeps failing because of the emergence of drug-resistant virus [28]. As a result, a mathematical model of the occurrence probability of drug-resistant virus species was created based on the trajectories of the state variables of HIV infection dynamic model. The stability analysis of ART in HIV/AIDS treatment dynamics was discussed in [29–31]. Moreover, the effect of singular and non-singular derivative of dynamical system refers to the studies in [32, 33]. The fractional derivative, Caputo–Fabrizio fractional derivative are all studied in [34–36]. The Genocchi polynomials are employed to a wavelet-based numerical scheme for fractional order SEIR epidemic of measles as in [37].

The organizing of this paper consists of four sections. In Sect. 1, we introduce the study of HIV–AIDS and also the last study for dynamical system of HIV–AIDS model. Our proposed model is provided in Sect. 2 by conducting two treatments of HAART and Immunotherapy. Moreover, the equilibria, basic reproduction number, positivity, boundedness, and stability of dynamical system are also presented in this section. Section 3 provides the numerical analysis of

our proposed model involving discretization step, stability, positivity, and consistency of numerical scheme. Moreover, we provide the validation results by establishing the fitting results between numerical results of our model and actual data. The three ARIMA models and neural network are also employed due to the significant results for optimization. The conclusions of all discussed problems are finally given in Sect. 4.

Remark 1 To the best our knowledge, the treatments of dynamical system in [38] are not studied. Due to the significant results of treatment, then we introduce two treatments of highly active antiretroviral therapy (HAART) and immunotherapy in our dynamical system. Moreover, the function of immune cell CTL $W(t)$ is introduced in this paper, where this immune cell CTL is able to destroy cells that produce viruses (infected CD4$^+$T cells).

2 Mathematical model

In this section, the dynamics of HIV–AIDS spread involving the populations of susceptible CD4$^+$T cells (U), infected CD4$^+$T cells (V), and immune cells CTL (W) are studied. Initially, we consider the following HIV–AIDS model with two treatments of highly active antiretroviral therapy (HAART) and immunotherapy

$$\begin{aligned}\frac{\mathrm{d}U}{\mathrm{d}t} &= \lambda - \mathrm{d}U - (1-u_1)\beta UV - u_2U,\\ \frac{\mathrm{d}V}{\mathrm{d}t} &= (1-u_1)\beta UV - (s+a)V,\\ \frac{\mathrm{d}W}{\mathrm{d}t} &= sV - bW + u_2U,\end{aligned} \tag{2.1}$$

where the parameters λ, β, d, a, s, and b, represent the rate of production for healthy CD4$^+$T cells, infection rate, natural mortality rate of healthy CD4$^+$T cells, natural mortality rate of infected CD4$^+$T cells, production rate of immune cell CTL, and natural mortality rate of immune cells CTL, respectively. Moreover, u_1 and u_2 represent the fixed parameters for highly active antiretroviral therapy (HAART) and Immunotherapy, respectively, where $0 \le (u_1, u_2) \le 1$. We consider that the HIV/AIDS can transmit over the time as well as the space, then the dynamical system (2.1) can be transformed into:

$$\begin{aligned}\frac{\partial U}{\partial t} &= D_1\frac{\partial^2 U}{\partial x^2} + \lambda - dU - (1-u_1)\beta UV - u_2U,\\ \frac{\partial V}{\partial t} &= D_2\frac{\partial^2 V}{\partial x^2} + (1-u_1)\beta UV - (s+a)V,\\ \frac{\partial W}{\partial t} &= D_3\frac{\partial^2 W}{\partial x^2} + sV - bW + u_2U,\end{aligned} \tag{2.2}$$

for $(x,t) \in \Omega \times [0, +\infty)$, the initial data,

$$\begin{aligned}&U(x,0) = U_0,\ V(x,0) = V_0,\\ &W(x,0) = W_0,\ x \in \Omega,\end{aligned} \tag{2.3}$$

and the no-flux homogeneous Neumann boundary conditions

$$\begin{aligned}\frac{\partial U(x,t)}{\partial n} &= \frac{\partial V(x,t)}{\partial n} = \frac{\partial W(x,t)}{\partial n} = 0,\\ &(x,t) \in \Sigma_T = \partial\Omega \times [0,T],\end{aligned} \tag{2.4}$$

where n is the Euclidean space.

2.1 Equilibria of dynamical system

This section provides the equilibria points and reproduction number $\mathcal{R}_0$. In epidemiology, the basic reproduction number $\mathcal{R}_0$ of an infection can be thought of as the number of cases produced by one case, on average during its infectious period, in an uninfected population [39]. This basic reproduction number is helpful to ensure that infectious disease can transmit or not in the population. If $\mathcal{R}_0 < 1$, the infection will stop in the long term. Moreover, if $\mathcal{R}_0 > 1$, the infection has the ability to transmit in the population. In general, if the $\mathcal{R}_0$ value is greater, then the control of epidemic is more difficult.

Theorem 2.1 *For all positive parameters, if $\mathcal{R}_0 < 1$, then the dynamical system (2.1) provides the disease-free equilibrium point $\mathcal{E}_0 = \left(\frac{\lambda}{d+u_2}, 0, \frac{\lambda u_2}{b(d+u_2)}\right)$. Moreover, the endemic equilibrium point $\mathcal{R}_0 > 1$ provides $\mathcal{E}_1 = \left(\frac{s+a}{(1-u_1)\beta}, \frac{u_2+d}{(1-u_1)\beta}(\mathcal{R}_0-1), \frac{s(u_2+d)}{b\beta(1-u_1)}(\mathcal{R}_0-1) + \frac{(s+a)u_2}{b\beta(1-u_1)}\right)$, where the basic reproduction number is defined as $\mathcal{R}_0 = \frac{\lambda\beta(1-u_1)}{(s+a)(d+u_2)}$.*

Proof The equilibrium points are obtained by considering $\frac{\mathrm{d}U}{\mathrm{d}t} = \frac{\mathrm{d}V}{\mathrm{d}t} = \frac{\mathrm{d}W}{\mathrm{d}t} = 0$ in the Eq. (2.1),

$$\begin{aligned}0 &= \lambda - \mathrm{d}U - (1-u_1)\beta UV - u_2U,\\ 0 &= (1-u_1)\beta UV - (s+a)V,\\ 0 &= sV - bW + u_2U.\end{aligned} \tag{2.5}$$

In the steady states, there are disease free and endemic equilibrium points. Then, we consider $V = 0$ in Eq. (2.5) to provide for both the disease free and endemic equilibrium points of this HIV–AIDS model:

$$\mathcal{E}_0 = (U^0, V^0, W^0) = \left(\frac{\lambda}{d+u_2}, 0, \frac{\lambda u_2}{b(d+u_2)}\right), \tag{2.6}$$

and

$$\mathcal{E}_1 = (U^*, V^*, W^*), \tag{2.7}$$

where

$$U^* = \frac{s+a}{(1-u_1)\beta},$$
$$V^* = \frac{u_2+d}{(1-u_1)\beta}(\mathcal{R}_0 - 1),$$
$$W^* = \frac{s(u_2+d)}{b\beta(1-u_1)}(\mathcal{R}_0 - 1) + \frac{(s+a)u_2}{b\beta(1-u_1)}.$$

It follows from $(2.1)_2$ at the disease free equilibrium point $\mathcal{E}_0$ ($V^0 = 0$) and the positivity of derivative in t of state variable V, one can derive

$$\Leftrightarrow \frac{\mathrm{d}V}{\mathrm{d}t} = (1-u_1)\beta U^0 V^0 - (s+a)V^0 > 0,$$
$$\Leftrightarrow (1-u_1)\beta U^0 > (s+a),$$
$$\Leftrightarrow \frac{\lambda\beta(1-u_1)}{(s+a)(d+u_2)} > 1.$$

Hence, the reproduction number $\mathcal{R}_0$ is obtained

$$\mathcal{R}_0 = \frac{\lambda\beta(1-u_1)}{(s+a)(d+u_2)} > 1. \tag{2.8}$$

□

Figure 1 shows the function of R_0 with the independent variables β and s. It is clear that R_0 increases as infection rate β increases and R_0 decreases as production rate of immune cell CTL s increases. The production rate of immune cell CTL is directly related to Immunotherapy. The most effective to control the HIV–AIDS spread is to control reproduction number R_0 less than one. Based on this principle, the strategy of immunotherapy's treatment should be advocated, so the body's immunity will be increased.

2.2 Positivity and boundedness of dynamical system

Theorem 2.2 *Suppose that $U(x,t)$, $V(x,t)$, and $W(x,t)$ be the solution of dynamical system (2.2) satisfying the initial data (2.3) and boundary conditions (2.4). Then, for $(x,t) \in \Omega \times [0,+\infty)$, $U(x,t)$, $V(x,t)$, and $W(x,t)$ are uniformly bounded, i.e.,*

$$\limsup_{x\in\Omega, t\to+\infty} (U,V,W)(x,t) \le \frac{\lambda}{a+b+d}.$$

Proof Let $\mathcal{P}(x,t) = (U+V+W)(x,t)$ be the total population. Then, by differentiating it in t, one has

$$\begin{aligned}\frac{\partial \mathcal{P}(x,t)}{\partial t} &= \frac{\partial U(x,t)}{\partial t} + \frac{\partial V(x,t)}{\partial t} + \frac{\partial W(x,t)}{\partial t} \\ &= (D_1+D_2+D_3)\frac{\partial^2 \mathcal{P}(x,t)}{\partial x^2} \\ &\quad + \lambda - (a+b+d)\mathcal{P}(x,t).\end{aligned}$$

Hence, by applying the boundary conditions (2.4), one can derive

$$\limsup_{x\in\Omega, t\to+\infty} \mathcal{P}(x,t) = \frac{\lambda}{a+b+d}.$$

We notice that $\mathcal{P}(x,t) = (U+V+W)(x,t)$, then we have

$$\limsup_{x\in\Omega, t\to+\infty} U(x,t) \le \limsup_{x\in\Omega, t\to+\infty} \mathcal{P}(x,t) = \frac{\lambda}{a+b+d}.$$

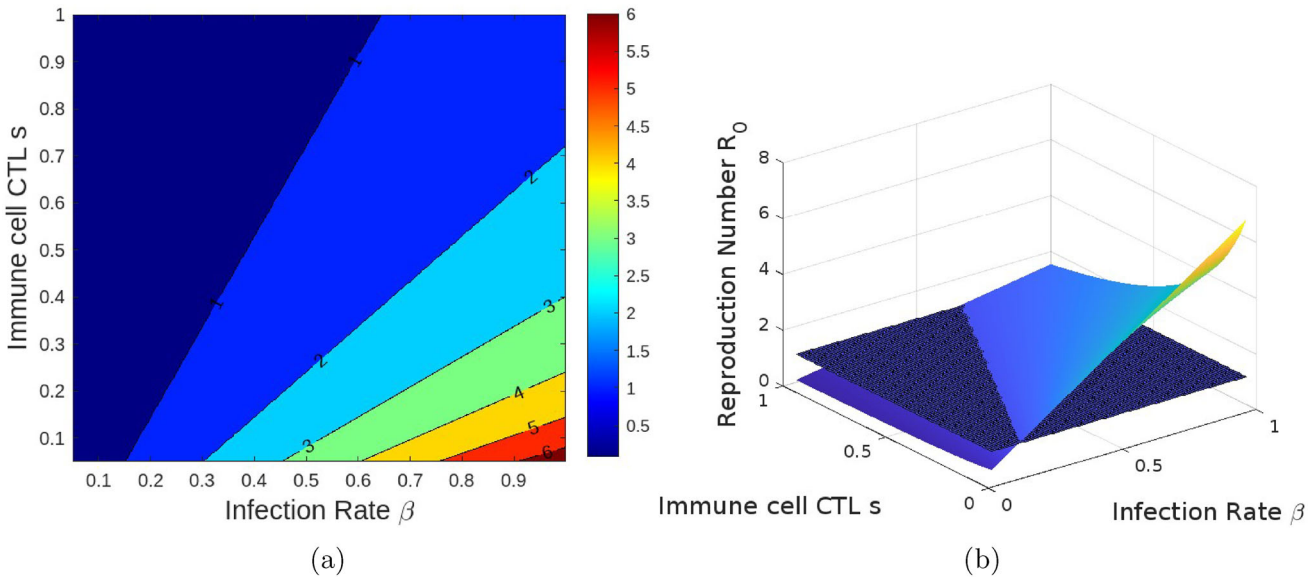

(a) (b)

Fig. 1 Tendency of R_0 with infection rate β and production rate of immune cell CTL s

The similar ways are employed into $V(x,t)$ and $W(x,t)$. Therefore, $U(x,t)$, $V(x,t)$, and $W(x,t)$ are uniformly bounded for $(x,t) \in \Omega \times [0,+\infty)$. □

Theorem 2.3 *Suppose that $U(x,t)$, $V(x,t)$, and $W(x,t)$ be the solution of dynamical system (2.2) satisfying the initial data (2.3) and boundary conditions (2.4). Then, for $(x,t) \in \Omega \times [0,+\infty)$, $U(x,t)$, $V(x,t)$, and $W(x,t)$ are non-negative.*

Proof By ignoring the diffusion terms, it follows from $(2.2)_1$, one has

$$\frac{\mathrm{d}U(t)}{\mathrm{d}t} + (\mathrm{d} + (1-u_1)\beta V)\, U(t) = \lambda.$$

We further integrate the above equation in t to get

$$\begin{aligned} U(t^*) = &\left(U(0) + \int_0^{t^*} \exp\left(\int_0^t \lambda\, (\mathrm{d} + (1-u_1) \right.\right. \\ &\left.\left. \times \beta V(\tau))\, V(\tau)\, \mathrm{d}\tau \right) \right) \\ &\exp\left(\int_0^t (\mathrm{d} + (1-u_1)\beta V(\tau))\ \mathrm{d}\tau \right)^{-1} \\ &\geq 0, \end{aligned}$$

for $t^* = \sup\{t \geq 0 : (U, V, W)(t) \geq 0\} \in [0,t]$. The similar arguments are employed to provide $(V, W)(t) \geq 0$. □

Then, we substitute Eq. (2.9) into (2.2) to get

$$\begin{aligned} &\sum_k \left(\mathcal{P}_{11} - D_1k^2 - \phi\right) U_k + \sum_k \mathcal{P}_{12} V_k + \sum_k \mathcal{P}_{13} W_k = 0, \\ &\sum_k \mathcal{P}_{21} U_k + \sum_k \left(\mathcal{P}_{22} - D_2k^2 - \phi\right) V_k + \sum_k \mathcal{P}_{23} W_k = 0, \\ &\sum_k \mathcal{P}_{31} U_k + \sum_k \mathcal{P}_{32} V_k + \sum_k \left(\mathcal{P}_{33} - D_3k^2 - \phi\right) W_k = 0. \end{aligned} \tag{2.10}$$

It follows from (2.10), one has the following matrix

$$J = \begin{pmatrix} \mathcal{P}_{11} - D_1k^2 - \phi & \mathcal{P}_{12} & \mathcal{P}_{13} \\ \mathcal{P}_{21} & \mathcal{P}_{22} - D_2k^2 - \phi & \mathcal{P}_{23} \\ \mathcal{P}_{31} & \mathcal{P}_{32} & \mathcal{P}_{33} - D_3k^2 - \phi \end{pmatrix} \tag{2.11}$$

where

$$\begin{aligned} &\mathcal{P}_{11} = -(d + (1-u_1)\beta V + u_2), \\ &\mathcal{P}_{12} = -(1-u_1)\beta U,\ \mathcal{P}_{13} = 0, \\ &\mathcal{P}_{21} = (1-u_1)\beta V,\ \mathcal{P}_{22} = -((s+a) - (1-u_1)\beta U), \\ &\mathcal{P}_{23} = 0, \\ &\mathcal{P}_{31} = u_2,\ \mathcal{P}_{32} = s,\ \mathcal{P}_{33} = -b. \end{aligned}$$

We substitute the disease-free equilibrium point $\mathcal{E}_0$ into (2.11), then one can derive

$$J(\mathcal{E}_0) = \begin{pmatrix} -(d + u_2 + D_1k^2 + \phi) & -(1-u_1)\beta U^0 & 0 \\ 0 & -((s+a) - (1-u_1)\beta U^0 + D_2k^2 + \phi) & 0 \\ u_2 & s & -(b + D_3k^2 + \phi) \end{pmatrix}. \tag{2.12}$$

2.3 Stability of dynamical system

In the next study, we provide the analysis of local and global stability for the disease-free and endemic equilibrium points as stated in the following theorems.

Theorem 2.4 *Suppose $\mathcal{R}_0 < 1$. Then, we can show that the equilibrium point $\mathcal{E}_0$ is locally asymptotical stable.*

Proof The local stability of dynamical system with the diffusion terms can be established by the strategy as introduced in [40, 41] by defining the following formula

$$\begin{aligned} U(x,t) &= \sum_k U_k e^{\phi t} \sin(kx), \\ V(x,t) &= \sum_k V_k e^{\phi t} \sin(kx), \\ W(x,t) &= \sum_k W_k e^{\phi t} \sin(kx). \end{aligned} \tag{2.9}$$

Applying the formula $|J(\mathcal{E}_0) - \lambda I_d| = 0$ into (2.12), then the eigenvalues satisfy the following characteristic equation

$$\begin{aligned} &(-(b + D_3k^2 + \phi) - \lambda)(-(d + u_2 + D_1k^2 + \phi) - \lambda) \\ &(-((s+a) - (1-u_1)\beta U^0 + D_2k^2 + \phi) - \lambda) = 0. \end{aligned} \tag{2.13}$$

It follows from (2.13), we notice that the eigenvalues $\lambda_1 = -(b + D_3k^2 + \phi) < 0$ and $\lambda_2 = -(d + u_2 + D_1k^2 + \phi) < 0$. Then, we only need to make sure that $\lambda_3 = -((s+a) - (1-u_1)\beta U^0 + D_2k^2 + \phi) < 0$. By substituting U^0 in Theorem 2.1, one has

$$\begin{aligned} &\frac{\lambda\beta(1-u_1)}{d+u_2} - (s+a) - D_2k^2 - \phi \\ &\quad = (s+a)(\mathcal{R}_0 - 1) - D_2k^2 - \phi. \end{aligned}$$

Then, we can conclude that $\lambda_3 < 0$ only if $\mathcal{R}_0 < 1$. □

Theorem 2.5 *Suppose $\mathcal{R}_0 > 1$. Then, we can show that the equilibrium point $\mathcal{E}_1$ is locally asymptotical stable.*

Proof By employing the similar ways as in Theorem 2.4. At the endemic equilibrium point $\mathcal{E}_1$, one has

$$J(\mathcal{E}_1) = \begin{pmatrix} \mathcal{A} & -(1-u_1)\beta U^* & 0 \\ (1-u_1)\beta V^* & \mathcal{B} & 0 \\ u_2 & s & \mathcal{C} \end{pmatrix}. \tag{2.14}$$

where

$$\begin{aligned} \mathcal{A} &= -(d + (1-u_1)\beta V^* + u_2 + D_1 k^2 + \phi), \\ \mathcal{B} &= -((s+a) - (1-u_1)\beta U^* + D_2 k^2 + \phi), \\ \mathcal{C} &= -(b + D_3 k^2 + \phi). \end{aligned}$$

The formula $|J(\mathcal{E}_1) - \lambda I_d| = 0$ is employed into (2.14), then the characteristic equation provides the following eigenvalues

$$\begin{aligned} \lambda_1 &= -(b + D_3 k^2 + \phi) < 0, \\ \lambda_2 &= \frac{-(a + d + (1-u_1)\beta(V^* - U^*) + u_2 + (D_1 + D_2)k^2 + 2\phi) - \sqrt{\mathcal{D}}}{2}, \\ \lambda_3 &= \frac{-(a + d + (1-u_1)\beta(V^* - U^*) + u_2 + (D_1 + D_2)k^2 + 2\phi) + \sqrt{\mathcal{D}}}{2}, \end{aligned}$$

where

$$\begin{aligned} \mathcal{D} = {} & (a + d + (1-u_1)\beta(V^* - U^*) + u_2 + (D_1 + D_2)k^2 \\ & + 2\phi)^2 - 4[(d + (1-u_1)\beta V^* + u_2 + D_1 k^2 \\ & + \phi)((s+a) - (1-u_1)\beta U^* + D_2 k^2 + \phi) \\ & + (1-u_1)\beta V^*(1-u_1)\beta U^*]. \end{aligned}$$

Then, $\mathcal{D} > 0$ and hence, $\lambda_2 < 0$. Moreover, the eigenvalues $\lambda_{2,3}$ provide the stability criterion. The eigenvalues $\lambda_{2,3}$ will be real and negative if $\lambda_{2,3}$ satisfies

$$\lambda_2 + \lambda_3 < 0, \ \lambda_2 \cdot \lambda_3 > 0.$$

Therefore, it follows from $\mathcal{D}$, one can derive

$$\begin{aligned} \lambda_2 + \lambda_3 = {} & -(a + d + (1-u_1)\beta(V^* - U^*) + u_2 \\ & + (D_1 + D_2)k^2 + 2\phi) < 0, \\ \lambda_2 \cdot \lambda_3 = {} & \left(d + \frac{\lambda\beta(1-u_1)}{s+a} + D_1 k^2 + \phi\right)(D_2 k^2 + \phi) \\ & + (\lambda\beta(1-u_1) - (d+u_2)(s+a)) > 0. \end{aligned}$$

Based on the above results, all eigenvalues are negative real part. Thus, we can conclude that all eigenvalues satisfy Theorem 2.5. □

Theorem 2.6 *Suppose $\mathcal{R}_0 < 1$. Then, we can show that the equilibrium point $\mathcal{E}_0$ is globally asymptotical stable.*

Proof We consider the following Lyapunov function

$$L_{\mathcal{E}_0}(t) = \int_\Omega \left[U(x,t) - U^0 - U^0 \ln \frac{U(x,t)}{U^0} + \frac{V^2(x,t)}{2} \right] dx.$$

Then, differentiating the above equation in t and substituting the dynamical system (2.2) into the result, one can derive

$$\begin{aligned} \frac{dL_{\mathcal{E}_0}(t)}{dt} = {} & \int_\Omega \left[\left(1 - \frac{U^0}{U(x,t)}\right) \frac{\partial U(x,t)}{\partial t} \right. \\ & \left. + V(x,t) \frac{\partial V(x,t)}{\partial t} \right] dx \\ = {} & \int_\Omega \left[\left(1 - \frac{U^0}{U(x,t)}\right) (D_1 \Delta U(x,t) + \lambda - (d \right. \\ & \left. + u_2)\, U(x,t) - (1-u_1)\beta U(x,t) V(x,t) \right] dx \\ & + \int_\Omega \left[D_2 V(x,t) \Delta V(x,t) + (1-u_1)\beta U(x,t) \right. \\ & \left. \times\, V^2(x,t) - (s+a) V^2(x,t) \right] dx. \end{aligned} \tag{2.15}$$

By employing the equilibrium points as in Theorem 2.1 into (2.15), then one has

$$\begin{aligned} \frac{\mathrm{d}L_{\mathcal{E}_0}(t)}{\mathrm{d}t} \le {} & \int_\Omega \left[\left(1 - \frac{U^0}{U(x,t)}\right) (D_1 \Delta U(x,t) \right. \\ & \left. + (\mathrm{d} + u_2) U^0 - (\mathrm{d} + u_2) U(x,t)) \right] \mathrm{d}x \\ & + \int_\Omega \left[D_2 V(x,t) \Delta V(x,t) + \frac{(1-u_1)\lambda\beta}{d+u_2} \right. \\ & \left. \times V^2(x,t) - (s+a) V^2(x,t) \right] \mathrm{d}x. \end{aligned} \tag{2.16}$$

We notice that

$$\begin{aligned} 0 &= \int_{\partial\Omega} \frac{U_0}{U(x,t)} \nabla U(x,t) \cdot n \, \mathrm{d}x \\ &= \int_\Omega \mathrm{div} \left(\frac{U^0}{U(x,t)} \nabla U(x,t) \right) \mathrm{d}x \\ &= \int_\Omega \left(\frac{U^0}{U(x,t)} \Delta U(x,t) - U^0 \frac{|\nabla U(x,t)|^2}{U^2(x,t)} \right), \end{aligned}$$

$$
\begin{aligned}
0 &= \int_{\partial\Omega} V(x,t)\nabla V(x,t)\cdot n \,\mathrm{d}x \qquad (2.17)\\
&= \int_{\Omega} \mathrm{div}\,(V(x,t)\nabla V(x,t))\,dx\\
&= \int_{\Omega} \left(V(x,t)\Delta V(x,t) + |\nabla V(x,t)|^2\right),
\end{aligned}
$$

and

$$
\begin{aligned}
\int_{\Omega} \Delta U(x,t)\,\mathrm{d}x &= \int_{\partial\Omega} \frac{\partial U(x,t)}{\partial n}\,\mathrm{d}x = 0,\\
\int_{\Omega} \Delta V(x,t)\,\mathrm{d}x &= \int_{\partial\Omega} \frac{\partial V(x,t)}{\partial n}\,\mathrm{d}x = 0,
\end{aligned} \qquad (2.18)
$$

where the divergence theorem and boundary conditions in (2.4) have been applied. Substituting Eqs. (2.17) and (2.18) into Eq. (2.16), then one has

$$
\begin{aligned}
\frac{\mathrm{d}L_{\mathcal{E}_0}(t)}{\mathrm{d}t} &\le -(d+u_2)\int_{\Omega}\frac{(U-U^0)^2}{U(x,t)}\,\mathrm{d}x\\
&\quad -(s+a)\int_{\Omega}(1-\mathcal{R}_0)V^2(x,t)\,\mathrm{d}x\\
&\quad -D_1U^0\int_{\Omega}\frac{|\nabla U(x,t)|^2}{U^2(x,t)}\,\mathrm{d}x - \int_{\Omega}|V(x,t)|^2\,\mathrm{d}x\\
&\le -C\int_{\Omega}\Big((U(x,t)-U^0)^2 + (V(x,t)-0)^2\\
&\quad + |\nabla U(x,t)|^2 + |\nabla V(x,t)|^2\Big)\,\mathrm{d}x.
\end{aligned} \qquad (2.19)
$$

We can conclude that $\frac{\mathrm{d}L_{\mathcal{E}_0}(t)}{\mathrm{d}t} \le 0$ if $\mathcal{R}_0 < 1$. Moreover, it follows from the following Lemma, □

Lemma 1 *Assume that $\psi, \varphi \in C^1[c_1,\infty)$, $\varphi \ge 0$ and ψ is bounded from below. Then, the conditions of $\psi'(t) \le -c_2\varphi$ and $\varphi'(t) \le C$ in $[c_1,\infty)$ imply that $\lim_{t\to\infty}\varphi = 0$ for some constants c_1, c_2, C,*

where the detailed proof of this Lemma can be seen in [42]. Then, we have

$$
\lim_{t\to\infty}\int_{\Omega}\left[(U-U^0)^2 + (V-0)^2 + |\nabla U|^2 + |\nabla I|^2\right]\mathrm{d}x = 0.
$$

Moreover, we apply the following Poincaré inequality

$$
\int_{\Omega} c_1|U-\bar{U}|^2 \le |\nabla U|^2\,\mathrm{d}x, \quad \int_{\Omega} c_2|V-\bar{V}|^2 \le |\nabla V|^2\,\mathrm{d}x,
$$

to get

$$
\lim_{t\to\infty}\int_{\Omega}\left[(U-\bar{U})^2 + (V-\bar{V})^2\right]\mathrm{d}x = 0, \qquad (2.20)
$$

where $\bar{U} = \frac{1}{|\Omega|}\int_{\Omega} U(x,t)\,\mathrm{d}x$ and $\bar{V} = \frac{1}{|\Omega|}\int_{\Omega} V(x,t)\,\mathrm{d}x$. Hence,

$$
\begin{aligned}
|\Omega|(\bar{U}-U^0)^2 &= \int_{\Omega}\left[\bar{U}-U(x,t)+U(x,t)-U^0\right]^2\,\mathrm{d}x\\
&\le \int_{\Omega}\left[\bar{U}-U(x,t)\right]^2\,\mathrm{d}x\\
&\quad + \int_{\Omega}\left[U(x,t)-U^0\right]^2\,\mathrm{d}x\\
|\Omega|(\bar{V}-0)^2 &= \int_{\Omega}\left[\bar{V}-V(x,t)+V(x,t)-0\right]^2\,\mathrm{d}x\\
&\le \int_{\Omega}\left[\bar{V}-V(x,t)\right]^2\,\mathrm{d}x\\
&\quad + \int_{\Omega}\left[V(x,t)-0\right]^2\,\mathrm{d}x.
\end{aligned} \qquad (2.21)
$$

Therefore, one has $\bar{U}\to U^0$ as $t\to\infty$ and $\bar{V}\to 0$ as $t\to\infty$. It follows from Theorem 2.2, the dynamical system (2.2) is bounded. Moreover, one has

$$
\begin{aligned}
\lim_{n\to\infty}\|U(\cdot,t_n) - F_1(\cdot)\|_{C^2(\Omega)} &= 0,\\
\lim_{n\to\infty}\|V(\cdot,t_n) - F_2(\cdot)\|_{C^2(\Omega)} &= 0,
\end{aligned}
$$

for a subsequence t_n, and non-negative functions $F_1, F_2 \in C^2(\Omega)$. By employing (2.20)-(2.21), one provides $F_1 \equiv U^0$ and $F_2 \equiv 0$. Therefore,

$$
\begin{aligned}
\lim_{n\to\infty}\left\|U(\cdot,t_n) - U^0\right\|_{C^2(\Omega)} &= 0,\\
\lim_{n\to\infty}\|V(\cdot,t_n) - 0\|_{C^2(\Omega)} &= 0.
\end{aligned}
$$

Theorem 2.7 *Suppose $\mathcal{R}_0 > 1$. Then, we can show that the equilibrium point $\mathcal{E}_1$ is globally asymptotical stable.*

Proof Firstly, we provide the following Lyapunov function

$$
\begin{aligned}
L_{\mathcal{E}_1}(t) = \int_{\Omega}\Bigg[&U(x,t) - U^* - U^*\ln\frac{U(x,t)}{U^*} + V(x,t)\\
&- V^* - V^*\ln\frac{V(x,t)}{V^*}\Bigg]\mathrm{d}x.
\end{aligned}
$$

Then, differentiating the above equation in t and substituting the dynamical system (2.2) into the result, one can derive

$$
\begin{aligned}
\frac{\mathrm{d}L_{\mathcal{E}_1}(t)}{\mathrm{d}t} &= \int_{\Omega}\left[\left(1-\frac{U^*}{U(x,t)}\right)\frac{\partial U(x,t)}{\partial t}\right.\\
&\quad \left. + \left(1-\frac{V^*}{V(x,t)}\right)\frac{\partial V(x,t)}{\partial t}\right]\mathrm{d}x\\
&= \int_{\Omega}\left[\left(1-\frac{U^*}{U(x,t)}\right)(\lambda - (d+u_2)U(x,t)\right.\\
&\quad \left. - (1-u_1)\beta U(x,t)V(x,t))\right]\mathrm{d}x
\end{aligned}
$$

$$
\begin{aligned}
&+\int_\Omega \left[\left(1-\frac{V^*}{V(x,t)}\right)((1-u_1)\beta U(x,t)\right.\\
&\left.\times\ V(x,t)-(s+a)V(x,t))\right]\mathrm{d}x\\
&+\int_\Omega \left(1-\frac{U^*}{U(x,t)}\right)D_1\Delta U(x,t)\\
&+\int_\Omega \left(1-\frac{V^*}{V(x,t)}\right)D_2\Delta V(x,t). \qquad (2.22)
\end{aligned}
$$

By conducting the equilibrium points in Theorem 2.1, divergence theorem and boundary conditions (2.4) as in (2.17–2.18) into (2.22) and $\lambda = (d+u_2)U^* + (s+a)V^*$, then one has

$$
\begin{aligned}
\frac{\mathrm{d}L_{\mathcal{E}_1}(t)}{\mathrm{d}t} \le& -(d+u_2)\int_\Omega \frac{(U(x,t)-U^*)^2}{U(x,t)}\,\mathrm{d}x\\
&-(s+a)\int_\Omega \frac{(V(x,t)-V^*)^2}{V(x,t)}\\
&-D_1U^*\int_\Omega \frac{|\nabla U(x,t)|^2}{U^2(x,t)}\,\mathrm{d}x\\
&-D_2V^*\int_\Omega \frac{|\nabla V(x,t)|^2}{V^2(x,t)}\,\mathrm{d}x. \qquad (2.23)
\end{aligned}
$$

According to the equilibrium point $(s+a)V^* = (1-u_1)\beta U^*V^*$, then (2.23) becomes

$$
\begin{aligned}
\frac{\mathrm{d}L_{\mathcal{E}_1}(t)}{\mathrm{d}t} \le& -(d+u_2)\int_\Omega \frac{(U(x,t)-U^*)^2}{U(x,t)}\,\mathrm{d}x\\
&-(1-u_1)\beta U^*\int_\Omega \frac{(V(x,t)-V^*)^2}{V(x,t)}\\
&-D_1U^*\int_\Omega \frac{|\nabla U(x,t)|^2}{U^2(x,t)}\,\mathrm{d}x\\
&-D_2V^*\int_\Omega \frac{|\nabla V(x,t)|^2}{V^2(x,t)}\,\mathrm{d}x\\
\le& -CG(t), \qquad (2.24)
\end{aligned}
$$

where

$$
\begin{aligned}
G(t) = \int_\Omega \Big((U(x,t)-U^*)^2 + (V(x,t)-V^*)^2\\
+\ |\nabla U(x,t)|^2 + |\nabla V(x,t)|^2\Big)\,\mathrm{d}x.
\end{aligned}
$$

From the previous results, we can see that $\frac{\mathrm{d}L_{\mathcal{E}_1}(t)}{\mathrm{d}t} \le 0$ if $u_1 \in [0,1]$. According to Lemma 1, one has

$$
\begin{aligned}
\lim_{t\to\infty}\int_\Omega \left[(U-U^*)^2 + (V-V^*)^2 + |\nabla U|^2 + |\nabla V|^2\right]\mathrm{d}x\\
= 0.
\end{aligned}
$$

Applying the following Poincaré inequality

$$
\int_\Omega r_1|U-\bar{U}|^2 \le |\nabla U|^2\,\mathrm{d}x, \quad \int_\Omega r_2|V-\bar{V}|^2 \le |\nabla U|^2\,\mathrm{d}x,
$$

then one has

$$
\lim_{t\to\infty}\int_\Omega (U-\bar{U})^2\,\mathrm{d}x = 0, \quad \lim_{t\to\infty}\int_\Omega (V-\bar{V})^2\,\mathrm{d}x = 0, \qquad (2.25)
$$

where $\bar{U} = \frac{1}{|\Omega|}\int_\Omega U(x,t)\,\mathrm{d}x$ and $\bar{V} = \frac{1}{|\Omega|}\int_\Omega V(x,t)\,\mathrm{d}x$. Hence,

$$
\begin{aligned}
|\Omega|(\bar{U}-U^*)^2 &= \int_\Omega \left[\bar{U}-U(x,t)+U(x,t)-U^*\right]^2\,\mathrm{d}x\\
&\le \int_\Omega \left[\bar{U}-U(x,t)\right]^2\,\mathrm{d}x\\
&\quad+\int_\Omega \left[U(x,t)-U^*\right]^2\,\mathrm{d}x\\
|\Omega|(\bar{V}-V^*)^2 &= \int_\Omega \left[\bar{V}-V(x,t)+V(x,t)-V^*\right]^2\,\mathrm{d}x\\
&\le \int_\Omega \left[\bar{V}-V(x,t)\right]^2\,dx\\
&\quad+\int_\Omega \left[V(x,t)-V^*\right]^2\,\mathrm{d}x. \qquad (2.26)
\end{aligned}
$$

Therefore, one has $\bar{U} \to U^*$ as $t \to \infty$ and $\bar{V} \to V^*$ as $t \to \infty$. Moreover, one has

$$
\begin{aligned}
\lim_{n\to\infty}\|U(\cdot,t_n) - H_1(\cdot)\|_{C^2(\Omega)} = 0,\\
\lim_{n\to\infty}\|V(\cdot,t_n) - H_2(\cdot)\|_{C^2(\Omega)} = 0,
\end{aligned}
$$

for a subsequence t_n, and non-negative functions $H_1, H_2 \in C^2(\Omega)$. By employing (2.25–2.26), one provides $H_1 \equiv U^*$ and $H_2 \equiv V^*$. Therefore,

$$
\begin{aligned}
\lim_{n\to\infty}\left\|U(\cdot,t_n) - U^*\right\|_{C^2(\Omega)} = 0,\\
\lim_{n\to\infty}\left\|V(\cdot,t_n) - V^*\right\|_{C^2(\Omega)} = 0.
\end{aligned}
$$

□

3 Numerical analysis

The physical phenomenon can be represented into the system of differential equations to provide the further studies. The dynamical system involving the diffusion terms is more complicated to provide the analytical solutions. Therefore, the role of numerical technique is required in this case to establish the numerical solutions. The numerical techniques are employed to investigate the model's behavior. Although

these techniques do not provide an analytical solution to the model, they do assist us in studying the physical phenomenon of the model. Moreover, in mathematical epidemiology, a numerical technique with meaningful properties such as positivity, consistency, and population boundedness is required. For this purpose, we apply the standard finite difference providing the physical behavior of mathematical epidemiology.

3.1 Discretization step

In this paper, the standard finite difference scheme is employed for studying the behavior of our model. The standard finite difference ensures the model's positivity and boundedness, which are essential properties of the state variables. The numerical techniques provide the alternative to approximate the solutions of dynamical systems for both linear and nonlinear differential equations [43–45]. We firstly transform our continuous dynamical system into the discrete formulation. Moreover, the Taylor's series is the most effective method to provide the approximations. We now consider maximum values of space and time namely M and N. Moreover, the partitions $lb = x_0 < x_1 < x_2 < \cdots < x_M = ub$ and $0 = t_0 < t_1 < t_2 < \cdots < t_N = T$, respectively, with the step size of space $h = \frac{lb-ub}{M}$ and step size of time $k = \frac{T}{N}$ is the discretization results of the spatial interval of space $[lb, ub]$ over the time $[0, T]$. Moreover, $x_j = jh$ and $t_m = mk$ are the points of partitions, where $j \in [0, M]$ and $m \in [0, N]$. At the points of partitions $(x_j, t_m) = (jh, mk)$, we suppose that U_j^m, V_j^m, and W_j^m denote the approximations of $U(x,t)$, $V(x,t)$, and $W(x,t)$, respectively. We firstly define the forward and central finite difference for first derivative in time and second derivative in space, respectively, as shown below.

$$\frac{\partial \mathcal{K}}{\partial t} = \frac{\mathcal{K}_j^{m+1} - \mathcal{K}_j^m}{\Delta t},$$
$$\frac{\partial^2 \mathcal{K}}{\partial x^2} = \frac{\mathcal{K}_{j-1}^{m+1} - 2\mathcal{K}_j^{m+1} + \mathcal{K}_{j+1}^{m+1}}{(\Delta x)^2}.$$

The discretization result of compartment U in $(2.2)_1$ is

$$\begin{aligned}
\frac{U_j^{m+1} - U_j^m}{\Delta t} &= D_1 \frac{U_{j-1}^{m+1} - 2U_j^{m+1} + U_{j+1}^{m+1}}{(\Delta x)^2} + \lambda \\
&\quad - dU_j^{m+1} - (1-u_1)\beta U_j^{m+1} V_j^m - u_2 U_j^{m+1}, \\
U_j^{m+1} - U_j^m &= \frac{D_1 \Delta t}{(\Delta x)^2}\left(U_{j-1}^{m+1} - 2U_j^{m+1} + U_{j+1}^{m+1}\right) \\
&\quad + \Delta t\lambda - \Delta t d U_j^{m+1} - \Delta t(1-u_1) \\
&\quad \times \beta U_j^{m+1} V_j^m - \Delta t u_2 U_j^{m+1}. \\
-\nu_1 U_{j-1}^{m+1} &+ \left(1 + 2\nu_1 + \Delta t d + \Delta t(1-u_1)\beta V_j^m \right. \\
&\quad \left. + \Delta t u_2\right) U_j^{m+1} - \nu_1 U_{j+1}^{m+1} = U_j^m + \Delta t\lambda,
\end{aligned} \tag{3.1}$$

where

$$\nu_1 = \frac{D_1 \Delta t}{(\Delta x)^2}.$$

The similar ways for the compartment V in $(2.2)_2$, one has

$$\begin{aligned}
\frac{V_j^{m+1} - V_j^m}{\Delta t} &= D_2 \frac{V_{j-1}^{m+1} - 2V_j^{m+1} + V_{j+1}^{m+1}}{(\Delta x)^2} \\
&\quad -(s+a)V_j^{m+1} + (1-u_1)\beta U_j^m V_j^{m+1}, \\
V_j^{m+1} - V_j^m &= \frac{D_1 \Delta t}{(\Delta x)^2}\left(V_{j-1}^{m+1} - 2V_j^{m+1} + V_{j+1}^{m+1}\right) \\
&\quad -\Delta t(s+a)V_j^{m+1} + \Delta t(1-u_1)\beta U_j^m V_j^{m+1}. \\
&\quad -\nu_2 V_{j-1}^{m+1} + (1 + 2\nu_2 + \Delta t(s+a) \\
&\quad - \Delta t(1-u_1)\beta U_j^m\Big) V_j^{m+1} - \nu_2 V_{j+1}^{m+1} \\
&= V_j^m,
\end{aligned} \tag{3.2}$$

where

$$\nu_2 = \frac{D_2 \Delta t}{(\Delta x)^2}.$$

Moreover, the compartment W in $(2.2)_3$ is

$$\begin{aligned}
\frac{W_j^{m+1} - W_j^m}{\Delta t} &= D_3 \frac{W_{j-1}^{m+1} - 2W_j^{m+1} + W_{j+1}^{m+1}}{(\Delta x)^2} \\
&\quad -bW_j^{m+1} + sV_j^m + u_2 U_j^m \\
W_j^{m+1} - W_j^m &= \frac{D_3 \Delta t}{(\Delta x)^2}\left(W_{j-1}^{m+1} - 2W_j^{m+1} + W_{j+1}^{m+1}\right) \\
&\quad -\Delta t b W_j^{m+1} + \Delta t s V_j^m + \Delta t u_2 U_j^m. \\
&\quad -\nu_3 W_{j-1}^{m+1} + (1 + 2\nu_3 + \Delta t b)\, W_j^{m+1} \\
&\quad -\nu_3 W_{j+1}^{m+1} \\
&= W_j^m + \Delta t s V_j^m + \Delta t u_2 U_j^m,
\end{aligned} \tag{3.3}$$

where

$$\nu_3 = \frac{D_3 \Delta t}{(\Delta x)^2}.$$

3.2 Stability of numerical scheme

The main concern in approximations of dynamical system is the increase in round-off errors. In other words, the small changes of initial conditions can affect the results significantly. Moreover, if the difference between approximate and exact solutions is small, then such approximations are stable. Then, Von-Neumann method [46–50] is addressed to study the stability criterion of the standard finite difference. The

Von-Neumann method provides the characteristics of stability for the numerical results of proposed model. For this purpose, we provide the following Fourier series to break down the numerical error in the results of HIV–AIDS model. Then, the following Fourier series are substituted into Eq. (3.1)

$$\begin{aligned}
U_j^m &= \mathcal{G}_u^m e^{i\phi jh},\\
U_j^{m+1} &= \mathcal{G}_u^{m+1} e^{i\phi jh},\\
U_{j-1}^{m+1} &= \mathcal{G}_u^{m+1} e^{i\phi (j-1)h},\\
U_{j+1}^{m+1} &= \mathcal{G}_u^{m+1} e^{i\phi (j+1)h},
\end{aligned}$$

to get

$$\begin{aligned}
&-\nu_1 U_{j-1}^{m+1} + \Big(1 + 2\nu_1 + \Delta t d + \Delta t(1-u_1)\beta V_j^m\\
&\quad + \Delta t u_2\Big) U_j^{m+1} - \nu_1 U_{j+1}^{m+1} = U_j^m + \Delta t\lambda,\\
&-\nu_1 \mathcal{G}_u^{m+1} e^{i\phi (j-1)h} + \Big(1 + 2\nu_1 + \Delta t d + \Delta t(1-u_1)\\
&\quad \times \beta V_j^m + \Delta t u_2\Big) \mathcal{G}_u^{m+1} e^{i\phi jh}\\
&-\nu_1 \mathcal{G}_u^{m+1} e^{i\phi (j+1)h} = \mathcal{G}_u^m e^{i\phi jh}.
\end{aligned}$$

The above equation is divided by $\mathcal{G}_u^m e^{i\phi jh}$ for both sides; then, one has

$$\begin{aligned}
&-\nu_1 \mathcal{G}_u e^{-i\phi h} + \Big(1 + 2\nu_1 + \Delta t d + \Delta t(1-u_1)\beta V_j^m\\
&\quad + \Delta t u_2\Big) \mathcal{G}_u - \nu_1 \mathcal{G}_u e^{i\phi h} = 1,\\
&-\nu_1 \mathcal{G}_u \left(e^{-i\phi h} + e^{i\phi h}\right) + \Big(1 + 2\nu_1 + \Delta t d\\
&\quad + \Delta t(1-u_1)\beta V_j^m + \Delta t u_2\Big) \mathcal{G}_u = 1,\\
&-2\nu_1 \mathcal{G}_u \cos(\phi h) + \Big(1 + 2\nu_1 + \Delta t d + \Delta t(1-u_1)\\
&\quad \times \beta V_j^m + \Delta t u_2\Big) \mathcal{G}_u = 1,\\
&\left(-2\nu_1 + 4\nu_1 \sin^2\left(\frac{\phi h}{2}\right) + 1 + 2\nu_1 + \Delta t d\right.\\
&\quad \left. + \Delta t(1-u_1)\beta V_j^m + \Delta t u_2\right) \mathcal{G}_u = 1.
\end{aligned}$$

$$|\mathcal{G}_u| = \left|\frac{1}{4\nu_1 \sin^2\left(\frac{\phi h}{2}\right) + 1 + \Delta t(d+u_2) + \Delta t(1-u_1)\beta V_j^m}\right| < 1 \tag{3.4}$$

We further employ the same strategy for Eq. (3.2) by substituting

$$\begin{aligned}
V_j^m &= \mathcal{G}_v^m e^{i\phi jh},\\
V_j^{m+1} &= \mathcal{G}_v^{m+1} e^{i\phi jh},\\
V_{j-1}^{m+1} &= \mathcal{G}_v^{m+1} e^{i\phi (j-1)h},\\
V_{j+1}^{m+1} &= \mathcal{G}_v^{m+1} e^{i\phi (j+1)h}.
\end{aligned}$$

Then, one has:

$$\begin{aligned}
&-\nu_2 V_{j-1}^{m+1} + \Big(1 + 2\nu_2 + \Delta t(s+a) - \Delta t(1-u_1)\\
&\quad \times \beta U_j^m\Big) V_j^{m+1} - \nu_2 V_{j+1}^{m+1} = V_j^m,\\
&-\nu_2 \mathcal{G}_v^{m+1} e^{i\phi (j-1)h} + \Big(1 + 2\nu_2 + \Delta t(s+a)\\
&\quad - \Delta t(1-u_1)\beta U_j^m\Big) \mathcal{G}_v^{m+1} e^{i\phi jh}\\
&-\nu_2 \mathcal{G}_v^{m+1} e^{i\phi (j+1)h} = \mathcal{G}_v^m e^{i\phi jh}.
\end{aligned}$$

For the simplification, we further divide the above equation by $\mathcal{G}_v^m e^{i\phi jh}$ for both sides to obtain

$$\begin{aligned}
&-\nu_2 \mathcal{G}_v e^{-i\phi h} + \Big(1 + 2\nu_2 + \Delta t(s+a) - \Delta t(1-u_1)\\
&\quad \times \beta U_j^m\Big) \mathcal{G}_v - \nu_2 \mathcal{G}_v e^{i\phi h} = 1,\\
&-\nu_2 \mathcal{G}_v \left(e^{-i\phi h} + e^{i\phi h}\right) + \Big(1 + 2\nu_2 + \Delta t(s+a)\\
&\quad - \Delta t(1-u_1)\beta U_j^m\Big) \mathcal{G}_v = 1,\\
&-2\nu_2 \mathcal{G}_v \cos(\phi h) + \Big(1 + 2\nu_2 + \Delta t(s+a)\\
&\quad - \Delta t(1-u_1)\beta U_j^m\Big) \mathcal{G}_v = 1,\\
&\left(-2\nu_2 + 4\nu_2 \sin^2\left(\frac{\phi h}{2}\right) + 1 + 2\nu_2 + \Delta t(s+a)\right.\\
&\quad \left. - \Delta t(1-u_1)\beta U_j^m\right) \mathcal{G}_v = 1.
\end{aligned}$$

$$|\mathcal{G}_v| = \left|\frac{1}{4\nu_2 \sin^2\left(\frac{\phi h}{2}\right) + 1 + \Delta t(s+a) - \Delta t(1-u_1)\beta U_j^m}\right| < 1 \tag{3.5}$$

Moreover, by substituting the following equation

$$\begin{aligned}
W_j^m &= \mathcal{G}_w^m e^{i\phi jh},\\
W_j^{m+1} &= \mathcal{G}_w^{m+1} e^{i\phi jh},\\
W_{j-1}^{m+1} &= \mathcal{G}_w^{m+1} e^{i\phi (j-1)h},\\
W_{j+1}^{m+1} &= \mathcal{G}_w^{m+1} e^{i\phi (j+1)h},
\end{aligned}$$

into Eq. (3.3), one can derive

$$\begin{aligned}
&-\nu_3 W_{j-1}^{m+1} + (1 + 2\nu_3 + \Delta t b)\, W_j^{m+1} - \nu_3 W_{j+1}^{m+1}\\
&\quad = W_j^m + \Delta t s V_j^m,\\
&-\nu_3 \mathcal{G}_w^{m+1} e^{i\phi (j-1)h} + (1 + 2\nu_3 + \Delta t b)\, \mathcal{G}_w^{m+1} e^{i\phi jh}\\
&\quad - \nu_3 \mathcal{G}_w^{m+1} e^{i\phi (j+1)h} = \mathcal{G}_w^m e^{i\phi jh}.
\end{aligned}$$

The term $\mathcal{G}_w^m e^{i\phi jh}$ is employed into the above equation for division, and one gets

$$-\nu_3 \mathcal{G}_w e^{-i\phi h} + (1 + 2\nu_3 + \Delta t b)\, \mathcal{G}_w - \nu_3 \mathcal{G}_w e^{i\phi h} = 1,$$

$$
\begin{aligned}
&-\nu_3\mathcal{G}_w\left(e^{-i\phi h}+e^{i\phi h}\right)+(1+2\nu_3+\Delta tb)\,\mathcal{G}_w=1,\\
&-2\nu_3\mathcal{G}_w\cos(\phi h)+(1+2\nu_3+\Delta tb)\,\mathcal{G}_w=1,\\
&\left(-2\nu_3+4\nu_3\sin^2\left(\frac{\phi h}{2}\right)+1+2\nu_3+\Delta tb\right)\mathcal{G}_w=1.\\
&|\mathcal{G}_w|=\left|\frac{1}{4\nu_3\sin^2\left(\frac{\phi h}{2}\right)+1+\Delta tb}\right|<1 \qquad (3.6)
\end{aligned}
$$

3.3 Positivity of numerical scheme

The positivity property of numerical scheme was introduced in [50] by conducting M-matrix theory [45]. The positivity of numerical scheme has important role in mathematical epidemiology to provide their behavior. In this paper, the dynamical system consists of three sub-populations namely susceptible (U), infected (V), and immune cells CTL (W) sub-populations. Then, for each time $t > 0$, $U(x,t) > 0$, $V(x,t) > 0$, and $W(x,t) > 0$.

Theorem 3.1 *For all $k = 1, 2, 3, \ldots$ indicating the time period of dynamical system, then the systems (2.1–2.3) provide the positivity, i.e., $U^k > 0$, $V^k > 0$, and $W^k > 0$.*

Proof Initially, we rewrite the dynamical system (2.1–2.3) into the following matrices

$$
\begin{aligned}
&\mathcal{A}U^{k+1}=U^k,\\
&\mathcal{B}V^{k+1}=V^k,\\
&\mathcal{C}W^{k+1}=W^k.
\end{aligned} \qquad (3.7)
$$

The square matrices of $\mathcal{A}$, $\mathcal{B}$, and $\mathcal{C}$ are

$$
\mathcal{A}=\begin{pmatrix}
a_3 & a_1 & 0 & \cdots & \cdots & 0\\
a_4 & a_3 & a_2 & \ddots & & \vdots\\
0 & a_4 & a_3 & a_2 & \ddots & \vdots\\
\vdots & \ddots & \ddots & \ddots & \ddots & \vdots\\
\vdots & & \ddots & a_4 & a_3 & a_2\\
0 & \cdots & \cdots & 0 & a_5 & a_3
\end{pmatrix}, \qquad (3.8)
$$

$$
\mathcal{B}=\begin{pmatrix}
b_3 & b_1 & 0 & \cdots & \cdots & 0\\
b_4 & b_3 & b_2 & \ddots & & \vdots\\
0 & b_4 & b_3 & b_2 & \ddots & \vdots\\
\vdots & \ddots & \ddots & \ddots & \ddots & \vdots\\
\vdots & & \ddots & b_4 & b_3 & b_2\\
0 & \cdots & \cdots & 0 & b_5 & b_3
\end{pmatrix}, \qquad (3.9)
$$

$$
\mathcal{C}=\begin{pmatrix}
c_3 & c_1 & 0 & \cdots & \cdots & 0\\
c_4 & c_3 & c_2 & \ddots & & \vdots\\
0 & c_4 & c_3 & c_2 & \ddots & \vdots\\
\vdots & \ddots & \ddots & \ddots & \ddots & \vdots\\
\vdots & & \ddots & c_4 & c_3 & c_2\\
0 & \cdots & \cdots & 0 & c_5 & c_3
\end{pmatrix}, \qquad (3.10)
$$

where

$$
\begin{aligned}
&a_1=a_5=-2\nu_1,\ a_2=a_4=-\nu_1,\\
&\quad a_3=1+2\nu_1+\Delta td+\Delta t(1-u_1)\beta V_j^m-\Delta tu_2,\\
&b_1=b_5=-2\nu_2,\ b_2=b_4=-\nu_2,\\
&\quad b_3=1+2\nu_2+\Delta t(s+a)-\Delta t(1-u_1)\beta U_j^m,\\
&c_1=c_5=-2\nu_3,\ c_2=c_4=-\nu_3,\ c_3=1+2\nu_3+\Delta tb.
\end{aligned}
$$

Moreover, the column matrices of U^k, V^k, and W^k are

$$
\begin{aligned}
&U^k=U_j^m+\Delta t\lambda,\\
&V^k=V_j^m,\\
&W^k=W_j^m+\Delta tsV_j^m+\Delta u_2U_j^m.
\end{aligned}
$$

Here, M-matrix consists of the matrices $\mathcal{A}$, $\mathcal{B}$, and $\mathcal{C}$. Therefore, the above equations become

$$
\begin{aligned}
&U^{k+1}=\mathcal{A}^{-1}U^k,\\
&V^{k+1}=\mathcal{B}^{-1}V^k,\\
&W^{k+1}=\mathcal{C}^{-1}W^k.
\end{aligned} \qquad (3.11)
$$

We firstly suppose that U^k, V^k and W^k are positive. Further step, by conducting the M-matrix criterion, the positivity of U^{k+1}, V^{k+1} and W^{k+1} are satisfied. In view of mathematical induction principle, the proof of theorem is achieved. □

3.4 Consistency of numerical scheme

The consistency of the standard finite difference indicates how close the numerical scheme and the system of differential equations are, where the system of the numerical scheme is firstly approximated by Taylor's series as in [46–48].

Theorem 3.2 *Given a system of differential equations $\mathcal{P}g = f$ and finite difference scheme $\mathcal{P}_{\Delta x,\Delta t}h = f$. Then, the finite difference scheme is consistent with the system of differential equations if for any smooth function $\phi(x,t)$ satisfies*

$$\mathcal{P}_{\Delta x,\Delta t}\phi - \mathcal{P}\phi \to 0 \text{ as } (\Delta x, \Delta t) \to 0.$$

Proof It follows from (2.2), the operator $\mathcal{P}$ can be written as follows

$$\begin{aligned} &\mathcal{P}\phi(x,t) = \left(\frac{\partial}{\partial t} - D_i\frac{\partial^2}{\partial x^2}\right)\phi(x,t), \\ &\text{where } i = 1,2,3, \text{ and} \\ &\phi(x,t) = (U(x,t), V(x,t), W(x,t)). \end{aligned} \tag{3.12}$$

Moreover, we provide that

$$\begin{aligned} &\mathcal{P}_{\Delta x,\Delta t}\phi(x,t) = \frac{\phi_j^{m+1} - \phi_j^m}{\Delta t} - D_i\frac{\phi_{j-1}^{m+1} - 2\phi_j^{m+1} + \phi_{j+1}^{m+1}}{\Delta x^2}, \\ &\text{where } i = 1,2,3, \text{ and} \\ &\phi(x,t) = (U(x_j,t_m), V(x_j,t_m), W(x_j,t_m)). \end{aligned} \tag{3.13}$$

By conducting (3.12)-(3.13), let us define that

$$\begin{aligned} U_j^{m+1} &= U(x_j,t_m) + \frac{\Delta t}{1!}U_t(x_j,t_m) + \frac{(\Delta t)^2}{2!}U_{tt}(x_j,t_m) \\ &\quad + \frac{(\Delta t)^3}{3!}U_{ttt}(x_j,t_m) + \ldots \end{aligned}$$

$$\begin{aligned} U_{j-1}^{m+1} &= U(x_j,t_{m+1}) - \frac{\Delta x}{1!}U_x(x_j,t_{m+1}) + \frac{(\Delta x)^2}{2!}U_{xx} \\ &\quad \times (x_j,t_{m+1}) - \frac{(\Delta x)^3}{3!}U_{xxx}(x_j,t_{m+1}) \\ &\quad + \frac{(\Delta x)^4}{4!}U_{xxxx}(x_j,t_{m+1}) - \ldots. \\ &= \left(U(x_j,t_m) + \frac{\Delta t}{1!}U_t(x_j,t_m) + \frac{(\Delta t)^2}{2!}U_{tt}(x_j,t_m)\right. \\ &\quad \left. + \frac{(\Delta t)^3}{3!}U_{ttt}(x_j,t_m) + \ldots.\right) \\ &\quad - \frac{\Delta x}{1!}\left(U_x(x_j,t_m) + \frac{\Delta t}{1!}U_{xt}(x_j,t_m) + \frac{(\Delta t)^2}{2!}\right. \\ &\quad \left. \times\, U_{xtt}(x_j,t_m) + \frac{(\Delta t)^3}{3!}U_{xttt}(x_j,t_m) + \ldots.\right) \\ &\quad + \frac{(\Delta x)^2}{2!}\left(U_{xx}(x_j,t_m) + \frac{\Delta t}{1!}U_{xxt}(x_j,t_m)\right. \\ &\quad + \frac{(\Delta t)^2}{2!}U_{xxtt}(x_j,t_m) + \frac{(\Delta t)^3}{3!}U_{xxttt}(x_j,t_m) \\ &\quad \left. + \cdots\right) - \cdots \end{aligned}$$

$$\begin{aligned} U_{j+1}^{m+1} &= U(x_j,t_{m+1}) + \frac{\Delta x}{1!}U_x(x_j,t_{m+1}) + \frac{(\Delta x)^2}{2!}U_{xx} \\ &\quad \times (x_j,t_{m+1}) + \frac{(\Delta x)^3}{3!}U_{xxx}(x_j,t_{m+1}) \\ &\quad + \frac{(\Delta x)^4}{4!}U_{xxxx}(x_j,t_{m+1}) + \cdots \\ &= \left(U(x_j,t_m) + \frac{\Delta t}{1!}U_t(x_j,t_m) + \frac{(\Delta t)^2}{2!}U_{tt}(x_j,t_m)\right. \\ &\quad \left. + \frac{(\Delta t)^3}{3!}U_{ttt}(x_j,t_m) + \cdots\right) + \frac{\Delta x}{1!}\left(U_x(x_j,t_m)\right. \\ &\quad + \frac{\Delta t}{1!}U_{xt}(x_j,t_m) + \frac{(\Delta t)^2}{2!}U_{xtt}(x_j,t_m) \\ &\quad \left. + \frac{(\Delta t)^3}{3!}U_{xttt}(x_j,t_m) + \cdots\right) \\ &\quad + \frac{(\Delta x)^2}{2!}\left(U_{xx}(x_j,t_m) + \frac{\Delta t}{1!}U_{xxt}(x_j,t_m)\right. \\ &\quad + \frac{(\Delta t)^2}{2!}U_{xxtt}(x_j,t_m) + \frac{(\Delta t)^3}{3!}U_{xxttt}(x_j,t_m) \\ &\quad \left. + \cdots\right) + \cdots \end{aligned}$$

By substituting the above Taylor series into the following discretization of U

$$\begin{aligned} &\frac{U_j^{m+1} - U_j^m}{\Delta t} - D_1\frac{U_{j-1}^{m+1} - 2U_j^{m+1} + U_{j+1}^{m+1}}{(\Delta x)^2} - \lambda \\ &\quad + dU_j^{m+1} + (1-u_1)\beta U_j^{m+1}V_j^m + u_2U_j^{m+1} = 0, \end{aligned}$$

one has:

$$\begin{aligned} &\left(U_t(x_j,t_m) + \frac{\Delta t}{2!}U_{tt}(x_j,t_m) + \frac{(\Delta t)^2}{3!}U_{ttt}(x_j,t_m)\right. \\ &\quad \left. + \frac{(\Delta t)^3}{4!}U_{tttt}(x_j,t_m) + \cdots\right) - D_1\left(U_{xx}(x_j,t_m)\right. \\ &\quad + \frac{\Delta t}{1!}U_{xxt}(x_j,t_m) + \frac{(\Delta t)^2}{2!}U_{xxtt}(x_j,t_m) \\ &\quad \left. + \frac{(\Delta t)^3}{3!}U_{xxttt}(x_j,t_m) + \cdots\right) \\ &\quad - \frac{D_1(\Delta x)^2}{12}\left(U_{xxxx}(x_j,t_m) + \frac{\Delta t}{1!}U_{xxxxt}(x_j,t_m)\right. \\ &\quad \left. + \frac{(\Delta t)^2}{2!}U_{xxxxtt}(x_j,t_m) + \cdots\right) - \cdots \end{aligned}$$

$$-\lambda+(d+(1-u_1)\beta V(x_j,t_m)+u_2)\left(U(x_j,t_m)+\frac{\Delta t}{1!}U_t(x_j,t_m)+\frac{(\Delta t)^2}{2!}U_{tt}(x_j,t_m)+\cdots\right)=0.$$

By employing the limit $(\Delta x, \Delta t)\to 0$. Then, the following terms become

$$\begin{bmatrix}\left(\frac{\Delta t}{2!}U_{tt}(x_j,t_m)+\frac{(\Delta t)^2}{3!}U_{ttt}(x_j,t_m)+\frac{(\Delta t)^3}{4!}U_{tttt}(x_j,t_m)+\cdots\right)\\ -D_1\left(\frac{\Delta t}{1!}U_{xxt}(x_j,t_m)+\frac{(\Delta t)^2}{2!}U_{xxtt}(x_j,t_m)+\frac{(\Delta t)^3}{3!}U_{xxttt}(x_j,t_m)+\cdots\right)\\ -\frac{D_1(\Delta x)^2}{12}\left(U_{xxxx}(x_j,t_m)+\frac{\Delta t}{1!}U_{xxxxt}(x_j,t_m)+\frac{(\Delta t)^2}{2!}U_{xxxxtt}(x_j,t_m)+\cdots\right)\\ +(d+(1-u_1)\beta V(x_j,t_m)+u_2)\left(\frac{\Delta t}{1!}U_t(x_j,t_m)+\frac{(\Delta t)^2}{2!}U_{tt}(x_j,t_m)+\cdots\right)\end{bmatrix}\to 0.$$

Since

$$\frac{\partial U}{\partial t}=U_t(x_j,t_m),\ \frac{\partial U}{\partial x}=U_x(x_j,t_m),\ \frac{\partial^2 U}{\partial x^2}=U_{xx}(x_j,t_m),\ \frac{\partial^2 U}{\partial x\partial t}=U_{xt}(x_j,t_m),\ldots$$

one can derive

$$\begin{aligned}&\frac{U_j^{m+1}-U_j^m}{\Delta t}-D_1\frac{U_{j-1}^{m+1}-2U_j^{m+1}+U_{j+1}^{m+1}}{(\Delta x)^2}\\ &-\lambda+dU_j^{m+1}+(1-u_1)\beta U_j^{m+1}V_j^m+u_2U_j^{m+1}\\ &-\left(\frac{\partial U}{\partial t}-D_1\frac{\partial^2 U}{\partial x^2}-\lambda+(d+(1-u_1)\beta V+u_2)U\right)\\ &\times\to 0\ \text{ as }\ (\Delta x,\Delta t)\to 0.\end{aligned}\tag{3.14}$$

Thus, the scheme of compartment U is consistent. Moreover, the consistency is also achieved for the schemes of compartments V and W by using the similar ways. Then, one has

$$\begin{bmatrix}\left(\frac{\Delta t}{2!}V_{tt}(x_j,t_m)+\frac{(\Delta t)^2}{3!}V_{ttt}(x_j,t_m)+\frac{(\Delta t)^3}{4!}V_{tttt}(x_j,t_m)+\cdots\right)\\ -D_2\left(\frac{\Delta t}{1!}V_{xxt}(x_j,t_m)+\frac{(\Delta t)^2}{2!}V_{xxtt}(x_j,t_m)+\frac{(\Delta t)^3}{3!}V_{xxttt}(x_j,t_m)+\cdots\right)\\ -\frac{D_2(\Delta x)^2}{12}\left(V_{xxxx}(x_j,t_m)+\frac{\Delta t}{1!}V_{xxxxt}(x_j,t_m)+\frac{(\Delta t)^2}{2!}V_{xxxxtt}(x_j,t_m)+\cdots\right)\\ +((s+a)-(1-u_1)\beta U(x_j,t_m))\left(\frac{\Delta t}{1!}V_t(x_j,t_m)+\frac{(\Delta t)^2}{2!}V_{tt}(x_j,t_m)+\cdots\right)\end{bmatrix}\to 0,$$

and

$$\begin{bmatrix}\left(\frac{\Delta t}{2!}W_{tt}(x_j,t_m)+\frac{(\Delta t)^2}{3!}W_{ttt}(x_j,t_m)+\frac{(\Delta t)^3}{4!}W_{tttt}(x_j,t_m)+\cdots\right)\\ -D_3\left(\frac{\Delta t}{1!}W_{xxt}(x_j,t_m)+\frac{(\Delta t)^2}{2!}W_{xxtt}(x_j,t_m)+\frac{(\Delta t)^3}{3!}W_{xxttt}(x_j,t_m)+\cdots\right)\\ -\frac{D_3(\Delta x)^2}{12}\left(W_{xxxx}(x_j,t_m)+\frac{\Delta t}{1!}W_{xxxxt}(x_j,t_m)+\frac{(\Delta t)^2}{2!}W_{xxxxtt}(x_j,t_m)+\cdots\right)\\ +b\left(\frac{\Delta t}{1!}W_t(x_j,t_m)+\frac{(\Delta t)^2}{2!}W_{tt}(x_j,t_m)+\cdots\right)\end{bmatrix}\to 0,$$

implying that

$$\begin{aligned}&\frac{V_j^{m+1}-V_j^m}{\Delta t}-D_2\frac{V_{j-1}^{m+1}-2V_j^{m+1}+V_{j+1}^{m+1}}{(\Delta x)^2}\\ &+(s+a)V_j^{m+1}-(1-u_1)\beta U_j^mV_j^{m+1}\\ &-\left(\frac{\partial V}{\partial t}-D_2\frac{\partial^2 V}{\partial x^2}+((s+a)-(1-u_1)\beta U)V\right)\\ &\to 0\ \text{ as }\ (\Delta x,\Delta t)\to 0.\end{aligned}\tag{3.15}$$

and

$$\begin{aligned}&\frac{W_j^{m+1}-W_j^m}{\Delta t}-D_3\frac{W_{j-1}^{m+1}-2W_j^{m+1}+W_{j+1}^{m+1}}{(\Delta x)^2}\\ &+bW_j^{m+1}-sV_j^m-u_2U_j^m\\ &-\left(\frac{\partial W}{\partial t}-D_3\frac{\partial^2 W}{\partial x^2}+bW-sV-u_2U\right)\\ &\to 0\ \text{ as }\ (\Delta x,\Delta t)\to 0.\end{aligned}\tag{3.16}$$

Based on the results in Eqs. (3.14), (3.15), (3.16), we can conclude that $(\mathcal{P}_{\Delta x,\Delta t}-\mathcal{P})\phi(x,t)\to 0$ as $(\Delta x,\Delta t)\to 0$ for any smooth function $\phi(x,t)$. □

3.5 Example of numerical scheme

In this section, we perform the example of simulation for the discretization results of HIV–AIDS model. The following parameters are all assumed

$$\lambda=10,\ \beta=0.002,\ d=0.02,\ a=0.24,\ s=0.2,\ b=0.02,$$
$$D_1=0.01,\ D_2=0.01,\ D_3=0.01.$$

Moreover, the initial conditions in (2.2) and the combinations of two treatments (HAART, Immunotherapy) are given below

$$U(x,0)=20,\ V(x,0)=20,\ W(x,0)=2,$$
$$(u_1=0;u_2=0),\ (u_1=0.5;u_2=0),$$
$$(u_1=0;u_2=0.001),\ (u_1=0.5;u_2=0.001).$$

Figure 2 provides the comparison results of $(U, V, W)(x, t)$ between $(u_1, u_2) = (0.5, 0.001)$ (endemic stage) and $(u_1, u_2) = (0.5, 0.1)$ (disease-free stage). Although the two treatments (HAART and Immunotherapy) are employed to both stages with a certain level, the increase in treatment of Immunotherapy (u_2) is more effective in reducing the level of infected CD4$^+$T cell $V(x, t)$. Moreover, these results can also be seen from the basic reproduction number $(\mathcal{R}_0)$, namely $(\mathcal{R}_0 = 1.9841 > 1)$ for $(u_1, u_2) = (0.5, 0.001)$ and $(\mathcal{R}_0 = 0.3472 < 1)$ for $(u_1, u_2) = (0.5, 0.1)$. Figure 3 represents the comparisons between no treatment and HAART treatment $(u_1 = 0.5)$, no treatment and two treatments (HAART treatment $u_1 = 0.5$ and Immunotherapy treatment $u_2 = 0.001$), one treatment (HAART treatment $u_1 = 0.5$) and two treatments (HAART treatment $u_1 = 0.5$ and Immunotherapy treatment $u_2 = 0.001$). Based on those three conditions, no treatment, one treatment, and two treatments give the reproduction numbers $\mathcal{R}_0 = 4.1667$, $\mathcal{R}_0 = 2.0833$, and $\mathcal{R}_0 = 1.9841$, respectively. We can see that the smallest basic reproduction number is $\mathcal{R}_0 = 1.9841$ with two treatments at once (HAART and Immunotherapy). Then, followed by the second small basic reproduction number $\mathcal{R}_0 = 2.0833$ with only one treatment of HAART, and the biggest basic reproduction number is achieved with $\mathcal{R}_0 = 4.1667$ without any treatments. From these all experiments, we can conclude that the two combinations of treatment are the most effective which can be represented in Fig. 3.

The susceptible CD4$^+$T cell, infected CD4$^+$T cell, and immune cell CTL sub-populations are, respectively, represented in blue, green, and red in Fig. 3. Moreover, Fig. 3a represents the comparisons between sub-population without HAART and Immunotherapy (solid line) and sub-population only with HAART (dotted line). The comparisons between sub-population without HAART and Immunotherapy (solid line) and sub-population with HAART and Immunotherapy at once (dotted line) are shown in Fig. 3b. Moreover, Fig. 3a, b gives the same trend for the profiles of susceptible CD4$^+$T cell, infected CD4$^+$T cell, and immune cell CTL. After applying the only one treatment (only HAART) and two treatments (HAART and Immunotherapy), it has a significant impact in increasing susceptible CD4$^+$T cell (blue), decreasing infected CD4$^+$T cell (green), and decreasing immune cell CTL (red). During the period when the CTL cell immune response is effective, HAART treatment is less necessary, because in this case the immune system plays an important role in controlling the HIV–AIDS virus. So the decrease in HAART therapy depends on immune stimulation and the strength of the CTL immune cell system against the HIV–AIDS virus. Figure 3c provides the comparisons between sub-population only with HAART (solid line) and sub-population with HAART and Immunotherapy at once (dotted line). As shown in Fig. 3c, after two treatments strategies (at first only HAART and then a combination of HAART and Immunotherapy), it gives a significant effect that the two treatments strategies are more effective for immune cell CTL than the previous treatment strategies.

Based on the basic reproduction number stated in Eq. (2.8), the treatments of HAART (u_1) and immunotherapy (u_2) have significant role to make the value of $\mathcal{R}_0$ smaller, i.e., the higher the values of u_1, u_2 are, the smaller the value of $\mathcal{R}_0$ is. The varying values of $u_1 = u_2 = 0.001; 0.01; 0.1; 0.5; 0.7$ are listed in Table 1 and represented in Fig. 4a, b. If we correlate Table 1 and Fig. 4a, b, we can conclude that the increasing number of treatments with Immunotherapy causes the CD4$^+$T cell infection rate to decrease. The more sloping V profile indicates the smaller the basic reproduction number as well. Moreover, based on the results in Table 1 and Fig. 4a, b, by conducting the same varying values of u_1 and u_2, then the immunotherapy (u_2) is more effective than HAART (u_1) in reducing the infected CD4$^+$T cell, indicated by the decrease in basic reproduction number (by immunotherapy) is faster than the decrease in basic reproduction number (by HAART). This case is in line with the formula of basic reproduction number, where the parameter of immunotherapy (u_2) is as a divider in that formula. Moreover, we validate our dynamical system with the actual data by conducting the classical formula of least square technique written as

$$\mathrm{RMSE}(\mathcal{N}) = \sum_{k=1}^{M} (\mathcal{Y}_{\mathrm{pred}}(k) - \mathcal{Y}_{\mathrm{data}}(k)), \tag{3.17}$$

where M is the number of actual data, $\mathcal{Y}_{\mathrm{pred}}$ is the numerical result of our dynamical system, $\mathcal{Y}_{\mathrm{data}}$ is the actual data of HIV–AIDS taken for 2 years 7 months, and $\mathcal{N}$ is the unknown parameters of our dynamical system in (2.2). Moreover, our dynamical system in (2.2) is firstly represented as follows

$$\frac{\partial \mathcal{Y}(x,t)}{\partial t} = \frac{\partial \mathcal{Y}(x,t)}{\partial x^2} + \mathcal{F}(x, t, \mathcal{Y}, \mathcal{N}), \tag{3.18}$$

where Eq. (3.18) is approximated by the standard finite difference. Our goal is to minimize the objective function

$$\min_{\mathcal{N}} \ \mathrm{RMSE}(\mathcal{N}), \quad \text{subject to Eq. (3.18).} \tag{3.19}$$

The more detailed algorithm of parameter estimation can be addressed in [51], and the algorithm of optimization is in [52]. We divide the actual data into three regions as represented in Fig. 4c, where the largest infected profile is achieved in the region of 2nd year. The trend of infected profile for 2 years 7 months, it is initially increased in the region of first year and finally, decreased in the region of third year. The simulation results with the finite difference scheme (blue)

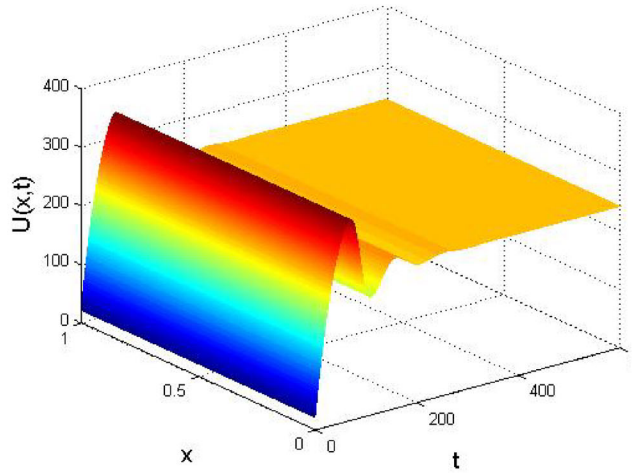

(a) Susceptible CD4$^+$T cell for $(u_1, u_2) = (0.5, 0.001)$

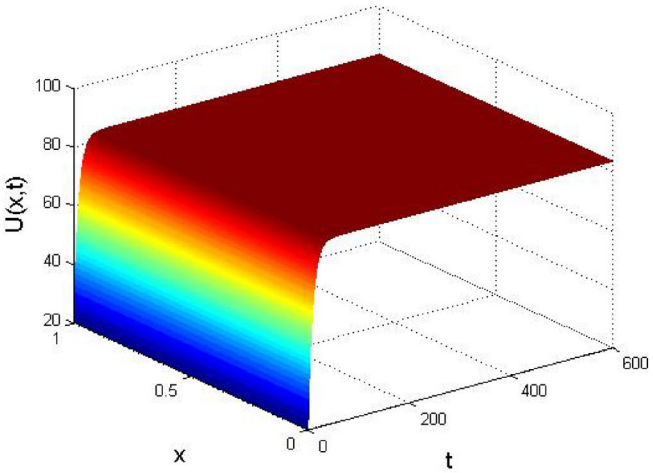

(b) Susceptible CD4$^+$T cell for $(u_1, u_2) = (0.5, 0.1)$

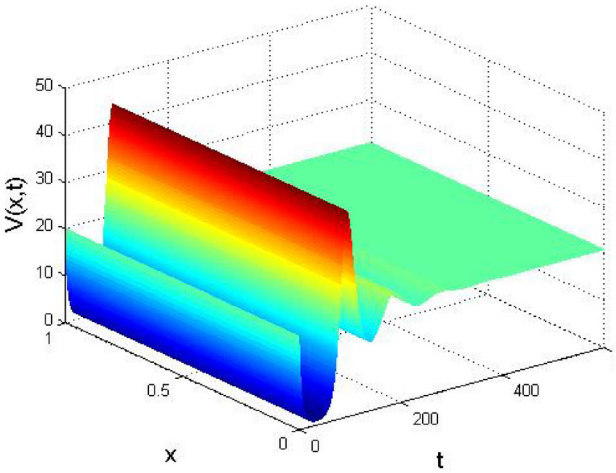

(c) Infected CD4$^+$T cell for $(u_1, u_2) = (0.5, 0.001)$

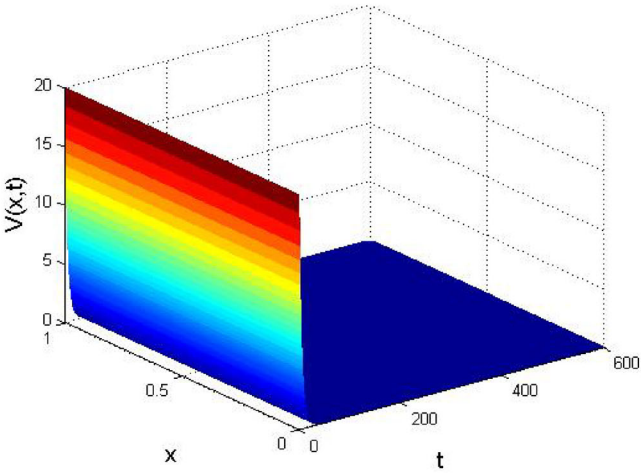

(d) Infected CD4$^+$T cell for $(u_1, u_2) = (0.5, 0.1)$

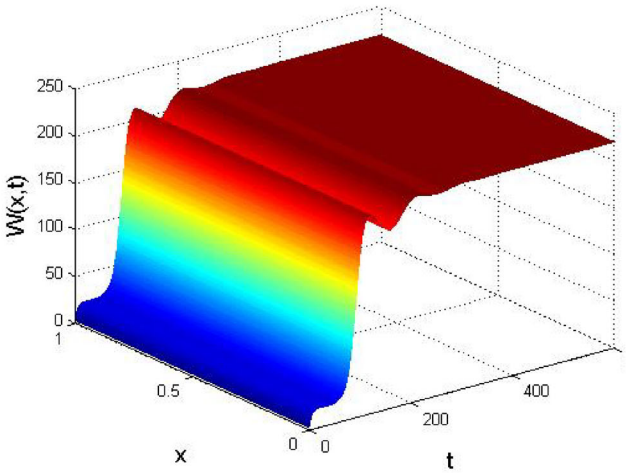

(e) Immune cell CTL for $(u_1, u_2) = (0.5, 0.001)$

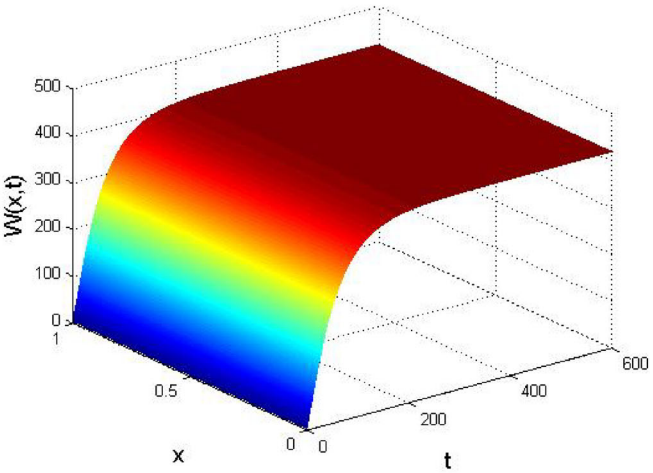

(f) Immune cell CTL for $(u_1, u_2) = (0.5, 0.1)$

Fig. 2 Profiles of $(U, V, W)(x, t)$ between endemic stage (left-hand side) and disease-free (right-hand side)

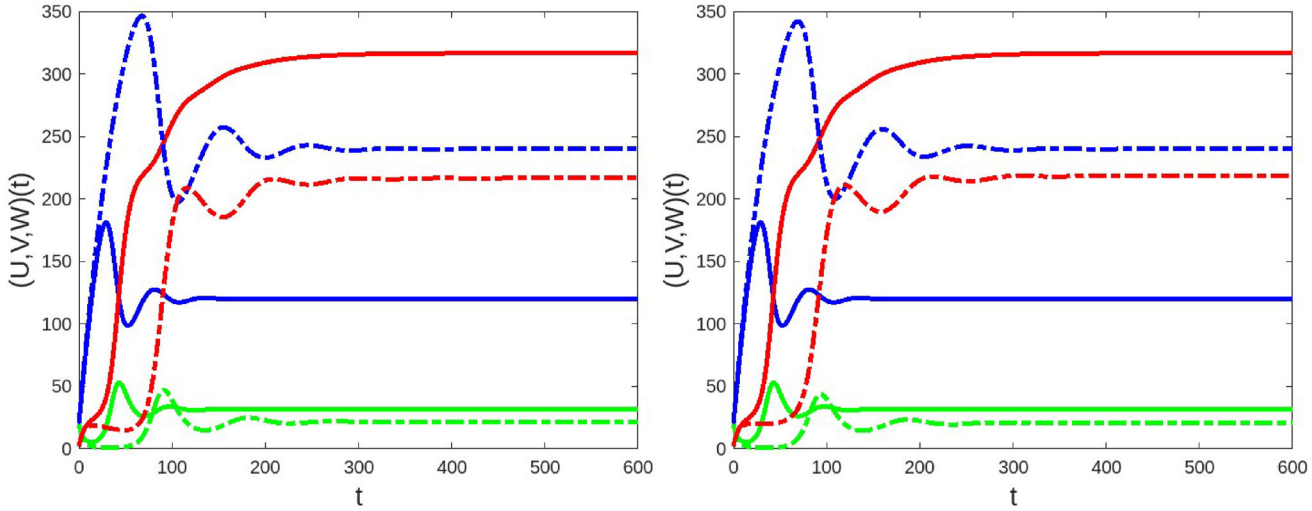

(a) $u_1 = 0, u_2 = 0$ (solid line) versus $u_1 = 0.5, u_2 = 0$ (dotted line)

(b) $u_1 = 0, u_2 = 0$ (solid line) versus $u_1 = 0.5, u_2 = 0.001$ (dotted line)

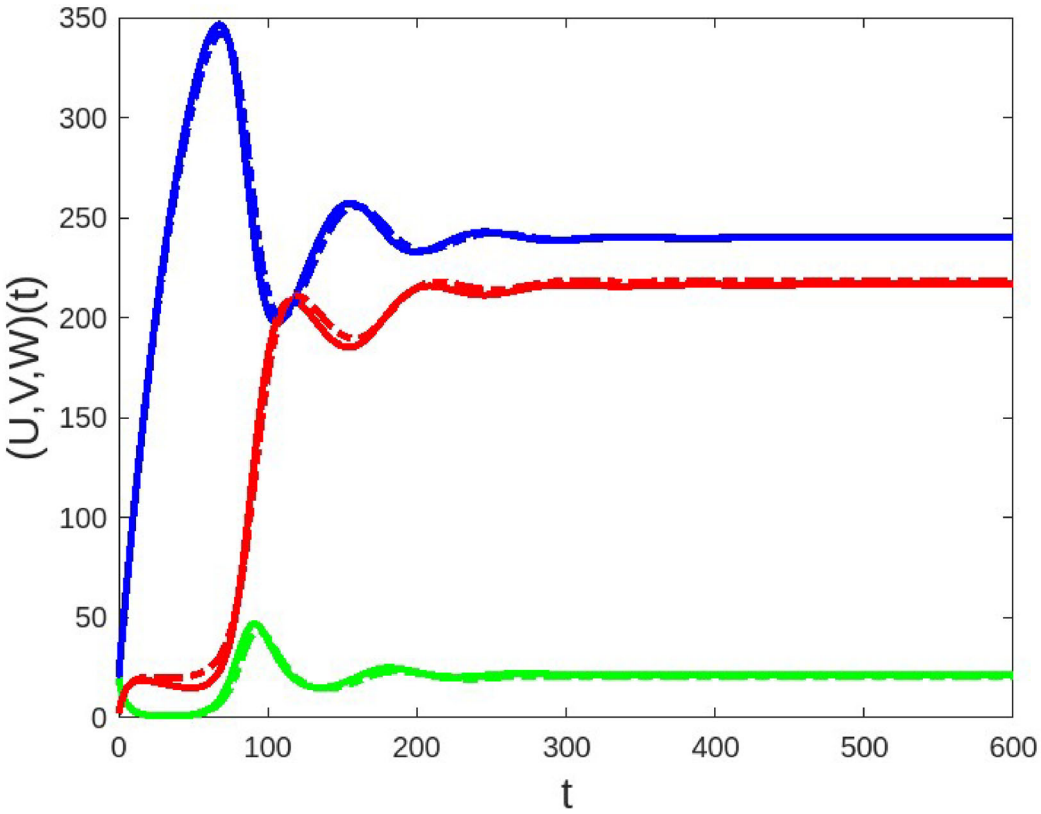

(c) $u_1 = 0.5, u_2 = 0$ (solid line) versus $u_1 = 0.5, u_2 = 0.001$ (dotted line)

Fig. 3 Profiles of $(U, V, W)(t)$ for varying values u_1 and u_2 (susceptible CD4$^+$T cell: blue, infected CD4$^+$T cell: green, immune cell CTL: red)

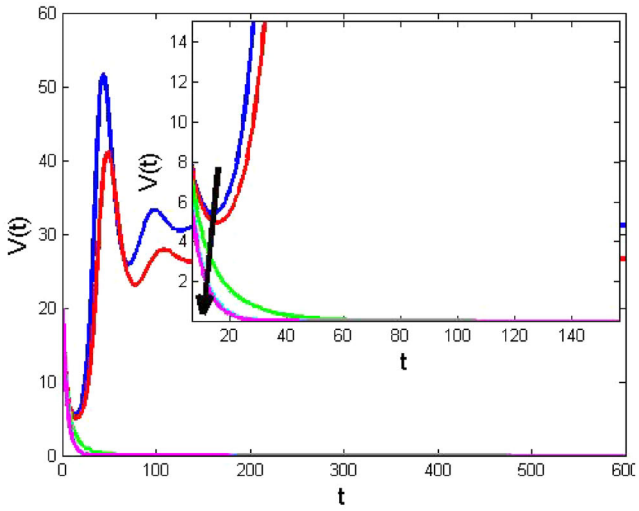

(a) varying u_2 and fixed $u_1 = 0.001$

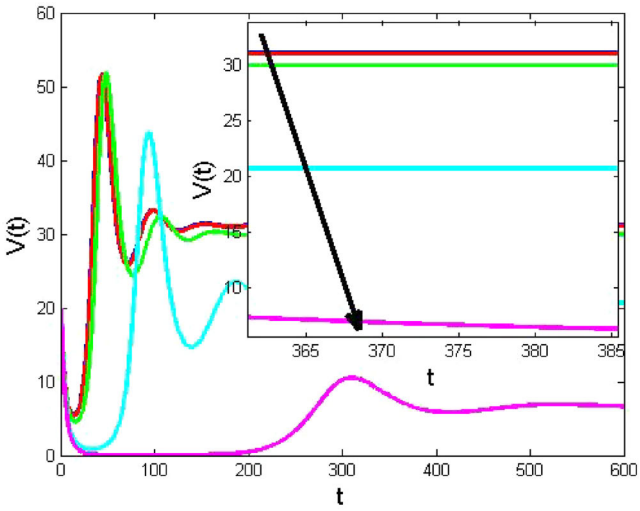

(b) varying u_1 and fixed $u_2 = 0.001$

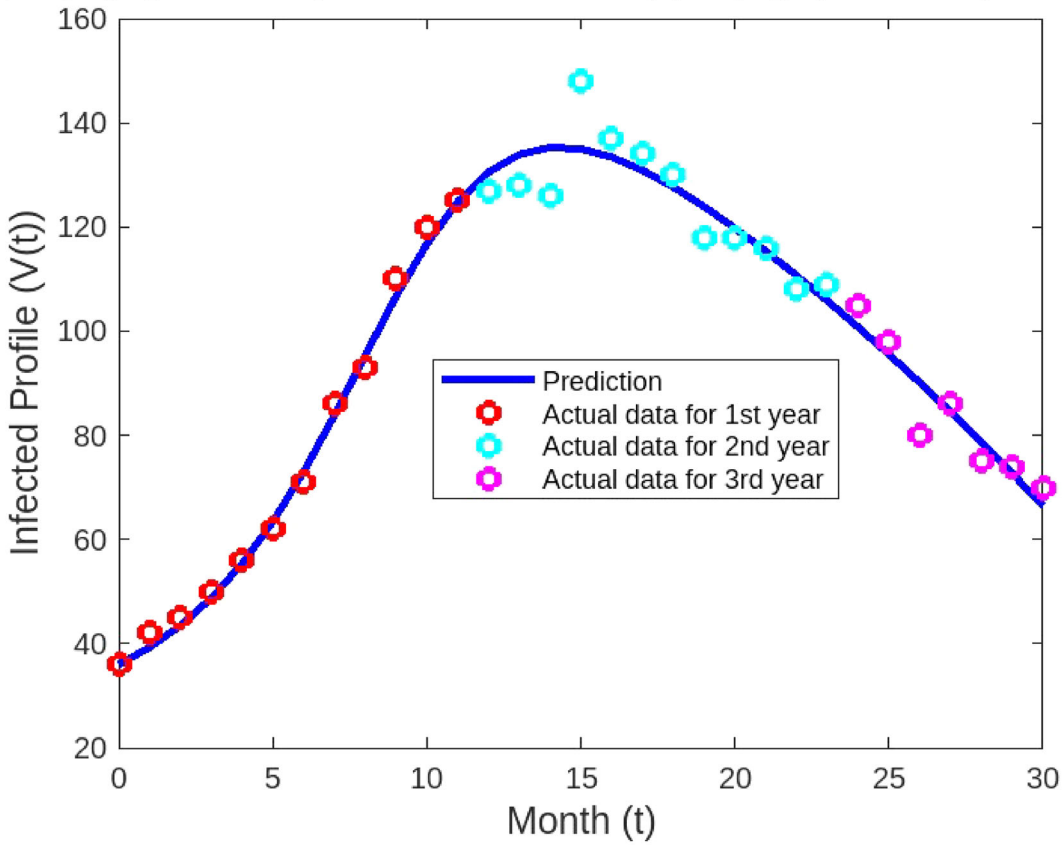

(c) Infected profile (prediction versus actual data)

Fig. 4 **a**, **b** Infected CD4$^+$T cell for varying immunotherapy and HAART, **c** prediction result and actual data of HIV–AIDS for 2 years 7 months

Table 1 Basic reproduction number for varying values of u_1 and u_2

u_2 (fixed $u_1 = 0.001$)	$\mathcal{R}_0$	u_1 (fixed $u_2 = 0.001$)	$\mathcal{R}_0$
0.001	3.9643	0.001	3.9643
0.01	2.7750	0.01	3.9286
0.1	0.6937	0.1	3.5714
0.5	0.1601	0.5	1.9841
0.7	0.1156	0.7	1.1905

Table 2 The z-test of coefficients

Model	Coef	Estimate	Std. error	z-Value	$P_r(>\|z\|)$
ARIMA(1,0,0)	ar1	0.98700	0.01694	58.2664	$<$ 2e−16
	intercept	80.34682	39.19259	2.0501	0.04036
ARIMA(1,0,1)	ar1	0.986622	0.017224	57.2804	$<$ 2.2e−16
	ma1	0.999984	0.122390	8.1705	3.071e−16
	intercept	78.807666	38.961383	2.0227	0.0431
ARIMA(1,1,0)	ar1	0.964592	0.034477	27.978	$<$ 2.2e−16

Table 3 The results of RMSE, MAE, MPE, MAPE, and MASE

Model	RMSE	MAE	MPE	MAPE	MASE
ARIMA(1,0,0)	6.679914	5.672293	4.4374	7.232001	0.9885463
ARIMA(1,0,1)	3.382467	2.876334	2.334251	3.778232	0.5012769
ARIMA(1,1,0)	1.342137	1.209709	0.340242	1.395972	0.2108236

are closed enough to the actual data (red, cyan, magenta). This indicates that our dynamical system model is reliable enough to be used in predicting the spread of HIV–AIDS.

According to Fig. 4c, we also provide three possible ARIMA models, including ARIMA (1,0,0), ARIMA (1,0,1), and ARIMA (1,1,0). We only use 21 data of 31 total data in Fig. 4c as data training, where this data training is then used to predict next 10 data. Moreover, the coefficients significance test is presented in Table 2. We can show that all ARIMA models are significant, because the P_r-value is less than $\alpha = 0.05$. The model significance is checked by using Ljung–Box test which gives the p-values for the models of ARIMA (1,0,0), ARIMA (1,0,1), and ARIMA (1,1,0), respectively, p-value = 1.569e−06, p-value = 9.529e−07, and p-value = 1.362e−10 which all p-values are less than $\alpha = 0.05$. According to this Ljung–Box, the results are same with the coefficients significance test that all models are significant. Table 3 shows the results of RMSE, MAE, MPE, MAPE, and MASE for each ARIMA model. We can conclude that the ARIMA(1,1,0) has the smallest value for RMSE, MAE, MPE, MAPE, and MASE which indicates that ARIMA(1,1,0) is the best model than the other models. Moreover, in Fig. 5a, the ARIMA(1,1,0) model (magenta) is the closest one to the HIV–AIDS model (this result of HIV–AIDS model is obtained from the least-square technique shown in Fig. 4c) than the other models. According to the results in Table 3 and Fig. 5a, we choose the ARIMA(1,1,0) model to predict next 10 data as shown in Fig. 5b. By applying the ARIMA(1,1,0) model for the 21 training data, we can see that the prediction results (next 10 data) show the same trend (decreasing trend) with the trend of HIV–AIDS model (complete data of 31 data) and actual data. Based on these results, we can conclude that the ARIMA(1,1,0) is eligible to predict the infected profile of HIV–AIDS model of this paper. Due to the importance of optimization of neural network (NN) for dynamical system, we present the training process of NN to characterize the dynamical systems (2.2). The main goal of problem is to learn an update rule for the state spaces $\mathbf{Y}_{j,m}$, where $\mathbf{Y} = (U, V, W)$ at space x_j and time t_m. As in Fig. 6, we employ two hidden layers where for each hidden layers has 15 neurons. We can see that the results of standard finite difference are closed enough to the results of NN. Moreover, as in Fig. 7, the best validation performance is only 1.4834 at epoch 4, and the error histogram indicating the errors between target and predicted values after training a feedforward NN shows that the middle part has a bin corresponding to the error of −0.2435 and the height of that bin for training dataset lies below but near to 80 and validation and test dataset lies between 100 and 120. It means that many samples from the different datasets which have an error lies in that range. The regression of training, validation, and test between output and target has the significant results, which means that the fit is still on the track of data.

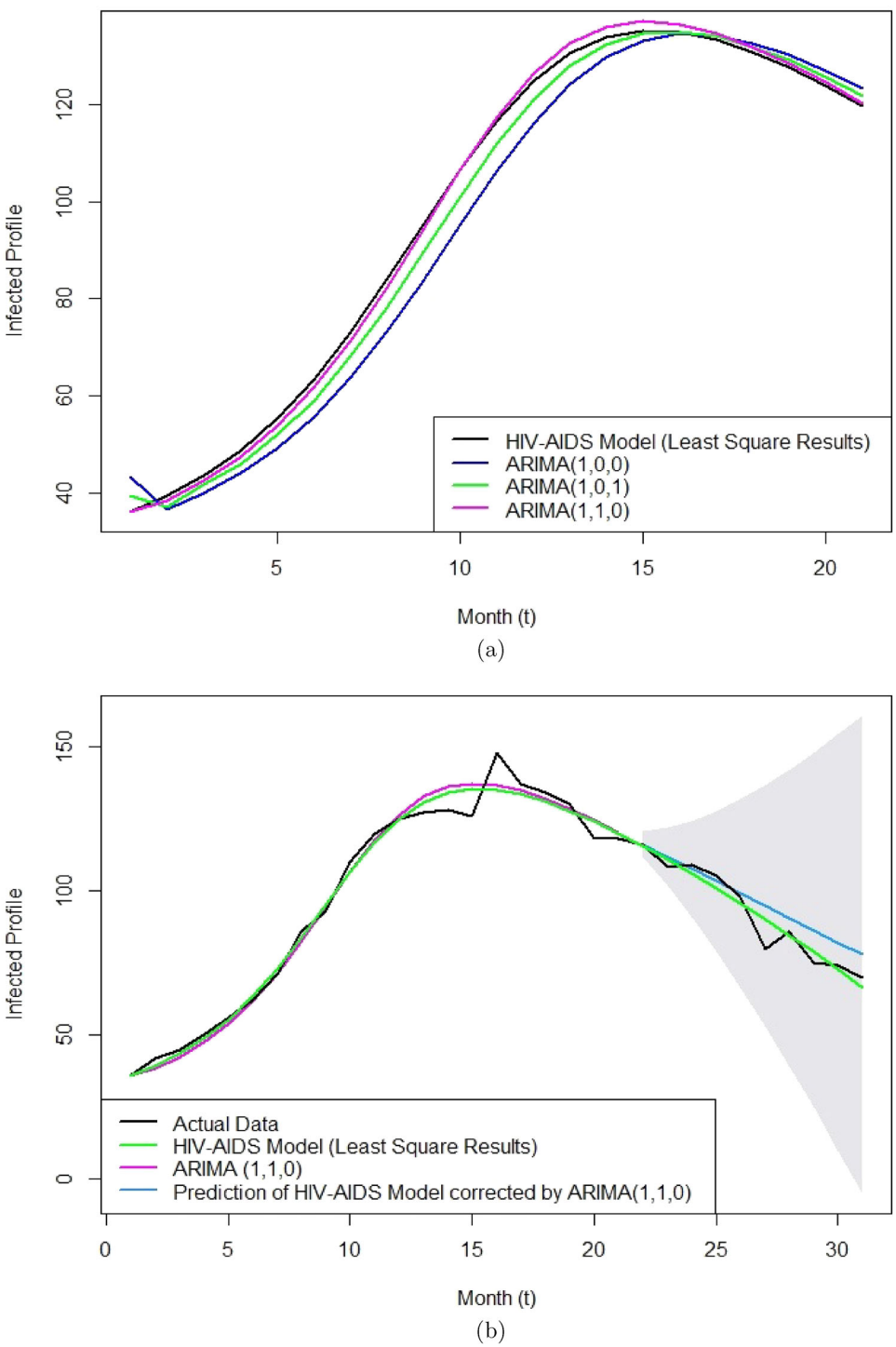

Fig. 5 **a** Fitting results for three ARIMA models, **b** prediction results by ARIMA(1,1,0) model

4 Conclusions

In this paper, we study the spatio-temporal HIV–AIDS model, where the change of system not only in time but also in space. The equilibrium points for disease-free and endemic are obtained by considering the diffusion parameters of D_1, D_2 and D_3 equal to zero. This condition also applies in providing the basic reproduction number ($\mathcal{R}_0$). The local stability of disease-free and endemic equilibrium points is established by definition of Fourier series, where the aim of using this Fourier series is because of the diffusion term. Moreover, we employ the standard finite difference to approximate our model into the numerical steps. The stability criterion of standard finite difference in our proposed

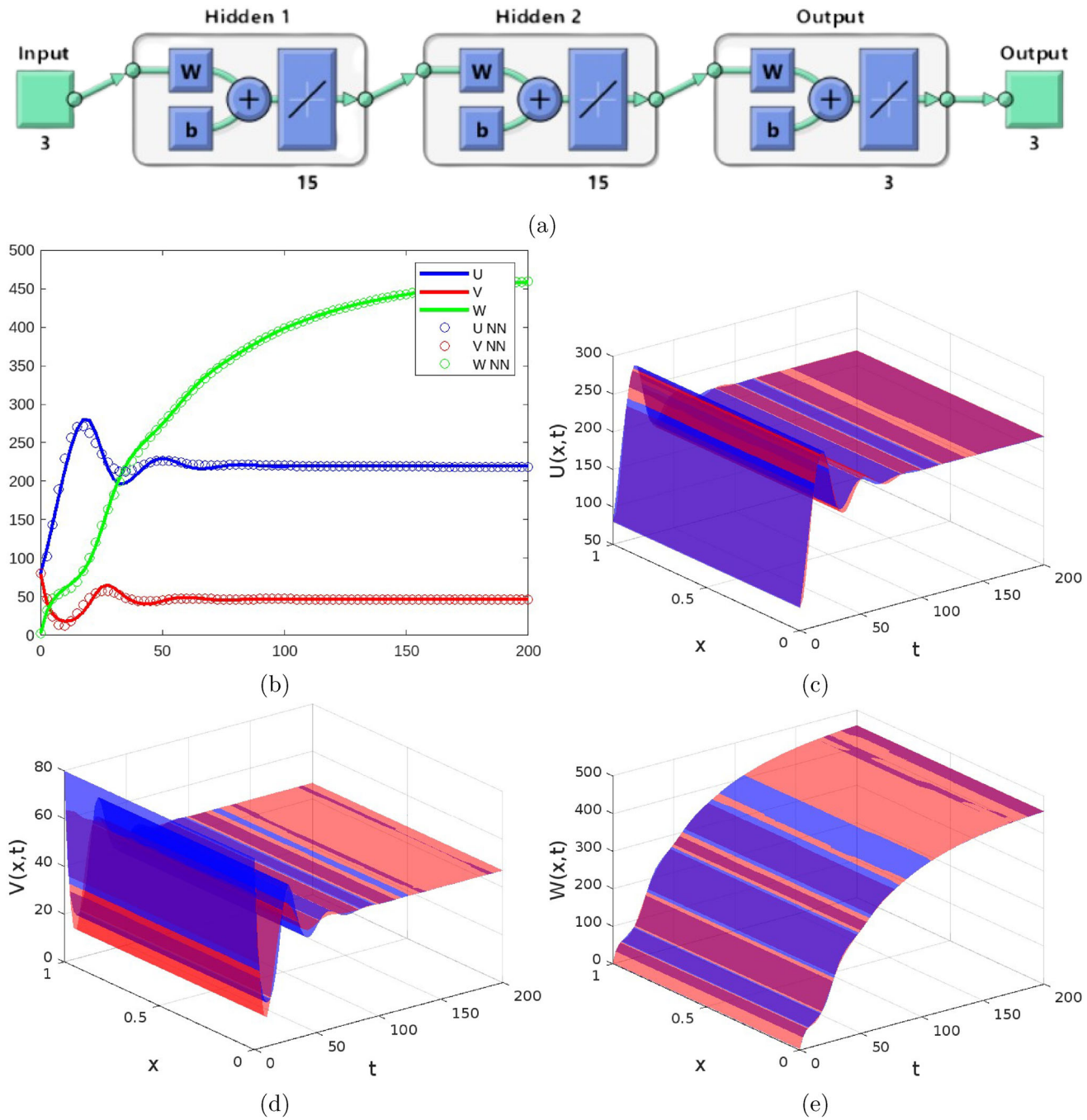

Fig. 6 Comparison results between standard finite difference and neural network (NN) for states of dynamical system U, V, W **b**: solid line (standard finite difference), circle (NN), **c**–**e**: blue surface (standard finite difference), red surface (NN)) with **a**: activation function $f(x) = x$, two hidden layers and 15 neurons for each hidden layer

model is established based on the standard way of using Von-Neumann stability. We can see that the stability criterion for standard finite difference of our model is less than 1, i.e., $|\mathcal{G}_u, \mathcal{G}_v, \mathcal{G}_w| < 1$. Moreover, the M-matrix theory is employed to provide the positivity of numerical scheme of our model. This technique only makes sure that there is no any negative population, i.e., susceptible CD4$^+$T, infected CD4$^+$T, and immune cell CTL sub populations. Meanwhile, knowing how close the numerical scheme of standard finite difference and the system of differential equations are, then consistency are employed. The experiment section is provided to know the effectiveness between HAART and

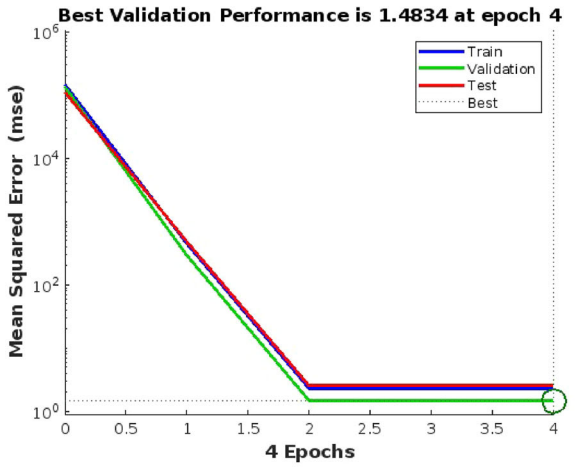

(a)

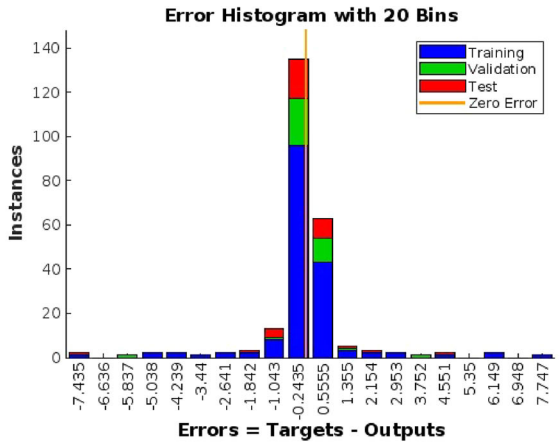

(b)

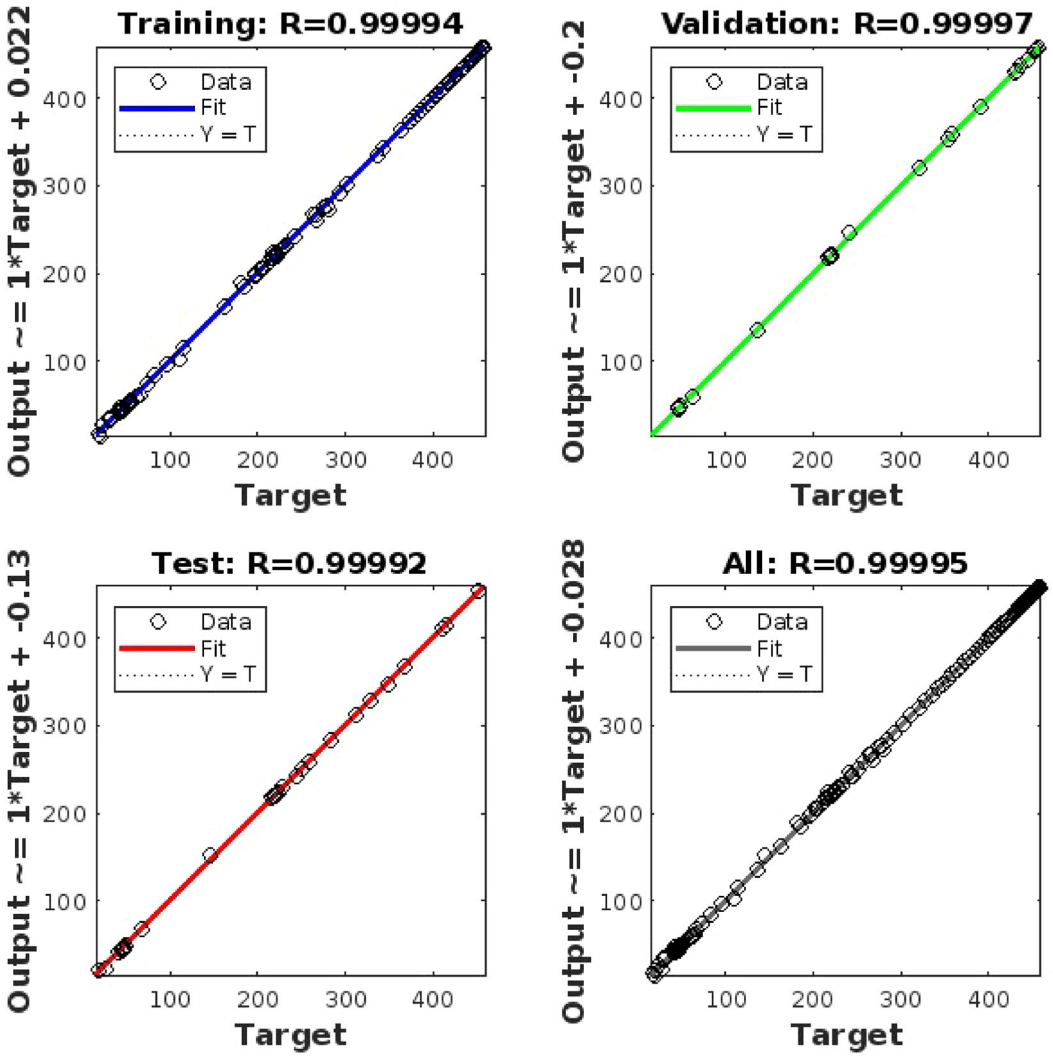

(c)

Fig. 7 Profiles of MSE, error histogram, and regression

Immunotherapy in reducing the infected CD4$^+$T cells. Based on the results, we can conclude that the treatment of HAART and Immunotherapy at once is the most efficient in decreasing the infected CD4$^+$T cells with the basic reproduction number ($\mathcal{R}_0 = 1.9841$). Moreover, based on the formula of basic reproduction number, the treatments of HAART and immunotherapy have significant role in reducing the infected CD4$^+$T cells, i.e., the higher the values of u_1 and u_2 are, the smaller the value of $\mathcal{R}_0$ is. By conducting the least square technique to our dynamical system, then our dynamical system is eligible to predict the spread of HIV–AIDS based on the validation results with the actual data. Moreover, we apply the ARIMA(1,1,0) model in this paper to predict infected profile and the result has the similar trend with the HIV–AIDS model (obtained from the least square technique) and the actual data. The reason for choosing ARIMA(1,1,0) model is because of the smallest value of RMSE (1.342137), MAE (1.209709), MPE (0.340242), MAPE (1.395972), and MASE (0.2108236). Moreover, due to the significant results (based on best validation performance, error histogram, and regression) of neural network for dynamical system, we employ the neural network for dynamical system with two hidden layers and 15 neurons for each hidden layer. The best validation performance is only 1.4834 at epoch 4, and the error histogram indicating the errors between target and predicted values after training a feedforward NN shows that the middle part has a bin corresponding to the error of -0.2435 and the height of that bin for training dataset lies below but near to 80 and validation and test dataset lies between 100 and 120. It means that many samples from the different datasets which have an error lie in that range.

Source code spatio-temporal model

```
clear all;clc;close all;
dt = 0.4;
dx = 0.05;
x = 0:dx:1;
t = 0:dt:600;
Nx = length(x);
Nt = length(t);
for i = 1:Nx
for j = 1:Nt
X(i,j) = x(i);
T(i,j) = t(j);
end
end
d1 = 0.01;
d2 = 0.01;
d3 = 0.01;
chs = {'1','2','3','4'};
ch = menu('Please choose
(1, 2, 3 or 4): ',chs);
if(ch==1)
u1 = 0; %HAART
u2 = 0; % Immunotherapy
ft = 'Without HAART & Immunotherapy';
elseif(ch==2)
u1 = 0.5; %HAART
u2 = 0; % Immunotherapy
ft = 'HAART Only';
elseif(ch==3)
u1 = 0; %HAART
u2 = 0.001; % Immunotherapy
ft = 'Immunotherapy Only';
else
% free–disease condition
u1 = 0.5; %HAART
u2 = 0.001; % Immunotherapy
ft = 'HAART & Immunotherapy';
end
%% parameters
lambda = 10;
beta = 0.002;
d = 0.02;
a = 0.24;
l = 0; % change from 0.001 to be 0
s = 0.2;
b = 0.02;
lambda1 = d1*dt/(dx^2);
lambda2 = d2*dt/(dx^2);
lambda3 = d3*dt/(dx^2);
%% initial condition
for i = 1:Nx
U(i,1)= 20;
end
for i = 1:Nx
V(i,1)= 20;
end
for i = 1:Nx
W(i,1)= 2;
end
%% main program
for k = 1:Nt–1
% matrik A
for i = 1:Nx
for j = 1:Nx
if(i==j)
A(i,j) = 1 + 2*lambda1 + dt*d
+ dt*(1–u1)*beta*V(i,k)
+ dt*u2;
elseif(j–i==1 && i==1)
A(i,j) = –2*lambda1;
elseif(j–i==1 && i>1)
```

```
A(i,j) = -lambda1;
elseif(i-j==1 && i<Nx)
A(i,j) = -lambda1;
elseif(i-j==1 && i==Nx)
A(i,j) = -2*lambda1;
else
A(i,j) = 0;
end
end
end
% matrik B
for i = 1:Nx
for j = 1:Nx
if(i==j)
B(i,j) = 1 + 2*lambda2
- dt*(1-u1)*beta*U(i,k)
+ dt*a +
dt*l*W(i,k);
elseif(j-i==1 && i==1)
B(i,j) = -2*lambda2;
elseif(j-i==1 && i>1)
B(i,j) = -lambda2;
elseif(i-j==1 && i<Nx)
B(i,j) = -lambda2;
elseif(i-j==1 && i==Nx)
B(i,j) = -2*lambda2;
else
B(i,j) = 0;
end
end
end
% matrik C
for i = 1:Nx
for j = 1:Nx
if(i==j)
C(i,j) = 1 + 2*lambda3 + dt*b;
elseif(j-i==1 && i==1)
C(i,j) = -2*lambda3;
elseif(j-i==1 && i>1)
C(i,j) = -lambda3;
elseif(i-j==1 && i<Nx)
C(i,j) = -lambda3;
elseif(i-j==1 && i==Nx)
C(i,j) = -2*lambda3;
else
C(i,j) = 0;
end
end
end
% boundary condition
for i = 1:Nx
BC_U(i,1) = U(i,k) + dt*lambda;
BC_V(i,1) = V(i,k);
BC_W(i,1) = W(i,k) + dt*s*V(i,k)
+ dt*u2*U(i,k);
end
U_new = inv(A)*BC_U;
V_new = inv(B)*BC_V;
W_new = inv(C)*BC_W;
for i = 1:Nx
U(i,k+1) = U_new(i,1);
V(i,k+1) = V_new(i,1);
W(i,k+1) = W_new(i,1);
end
end
figure(1)
g = surf(T,X,U)
ylabel('x','FontSize',14)
xlabel('t','FontSize',14)
zlabel('U(x,t)','FontSize',14)
%title('ENDEMIC EQUILIBRIUM',
'FontSize',14)
set(g,'LineStyle','none')
figure(2)
g = surf(T,X,V)
ylabel('x','FontSize',14)
xlabel('t','FontSize',14)
zlabel('V(x,t)','FontSize',14)
%title('ENDEMIC EQUILIBRIUM',
'FontSize',14)
set(g,'LineStyle','none')
figure(3)
g = surf(T,X,W)
ylabel('x','FontSize',14)
xlabel('t','FontSize',14)
zlabel('W(x,t)','FontSize',14)
%title('ENDEMIC EQUILIBRIUM',
'FontSize',14)
set(g,'LineStyle','none')
figure(4)
plot(t,U,'b-','LineWidth',2.4)
hold on
plot(t,V,'g-','LineWidth',2.4)
hold on
plot(t,W,'r-','LineWidth',2.4)
ylabel('(U,V,W)(t)','FontSize',14)
xlabel('t','FontSize',14)
%title('ENDEMIC EQUILIBRIUM',
'FontSize',14)
%% subplot
figure(5)
subplot(2,2,1)
g = surf(T,X,U)
set(g,'LineStyle','none')
zlabel('Uninfected U(x,t)','FontSize',14)
xlabel('Time (t)','FontSize',14)
```

```
ylabel('Space (x)','FontSize',14)
title(sprintf(ft),'FontSize',14)
subplot(2,2,2)
g = surf(T,X,V)
set(g,'LineStyle','none')
zlabel('Infected V(x,t)','FontSize',14)
xlabel('Time (t)','FontSize',14)
ylabel('Space (x)','FontSize',14)
title(sprintf(ft),'FontSize',14)

subplot(2,2,3)
g = surf(T,X,W)
set(g,'LineStyle','none')
zlabel('Immune Response W(x,t)',
'FontSize',14)
xlabel('Time (t)','FontSize',14)
ylabel('Space (x)','FontSize',14)
title(sprintf(ft),'FontSize',14)

subplot(2,2,4)
plot(t,U,'b','LineWidth',2.4)
hold on
plot(t,V,'g','LineWidth',2.4)
hold on
plot(t,W,'r','LineWidth',2.4)
ylabel('(U,V,W)(t)','FontSize',14)
xlabel('Time','FontSize',14)
title(sprintf(ft),'FontSize',14)

R0 = (lambda*beta*(1-u1))/(a*(d+u2))
```

Source Code NN

```
clc;clear all;close all
dt = 2.5;t = 0:dt:200;
lambda=25;beta=0.002;d=0.02;
a=0.24;s=0.2;b=0.02;
% u1=0;u2=0;
u1=0;u2=0.001;
% u1=0.05;u2=0;
% u1=0.05;u2=0.001;
HIV=@(t,x)([lambda-d*x(1)
-(1-u1)*beta*x(1)*x(2)-u2*x(1);...
(1-u1)*beta*x(1)*x(2)-(s+a)*x(2);...
s*x(2)-b*x(3)+u2*x(1)]);
ode_options=odeset('RelTol',1e
-10,'AbsTol',1e-11);
input=[];output=[];
x0=[80;80;2];
[t,y]=ode45(HIV,t,x0);
input=[input;y(1:end-1,:)];
output=[output;y(2:end,:)];
% plot3(y(:,1),y(:,2),y(:,3)), hold on
% plot3(x0(1),x0(2),x0(3),'ro')
figure(1)
plot(t,y(:,1),'b','LineWidth',2.0)
hold on
plot(t,y(:,2),'r','LineWidth',2.0)
hold on
plot(t,y(:,3),'g','LineWidth',2.0)
net=feedforwardnet([5 5]);
net.layers{1}.transferFcn='purelin';
net.layers{2}.transferFcn='purelin';
net=train(net,input.',output.');
ynn(1,:)=x0;
for jj=2:length(t)
y0=net(x0);
ynn(jj,:)=y0.';x0=y0;
end
hold on
plot(t,ynn(:,1),'bo')
hold on
plot(t,ynn(:,2),'ro')
hold on
plot(t,ynn(:,3),'go')
% plot3(ynn(:,1),ynn(:,2),ynn(:,3),':'
,'LineWidth',[2])
legend('U','V','W','U NN','V NN','W NN');
```

Author Contributions MG contributed to formal analysis, investigation, methodology, software, writing—original draft, and writing—review and editing.

Funding Mohammad Ghani received financial support for the research under Contract Number 121/UN3.1.17/PT/2022 by the Faculty of Advanced Technology and Multidiscipline, Universitas Airlangga, Indonesia.

Declarations

Conflict of interest None of the authors of this paper has a financial or personal relationship with other people or organizations that could inappropriately influence or bias the content of the paper. It is to specifically state that "No Competing interests are at stake and there is No Conflict of Interest" with other people or organizations that could inappropriately influence or bias the content of the paper.

References

1. Campbell EM, Jia H, Shankar A, Hanson D, Luo W, Masciotra S, Blosser SJ (2017) Detailed transmission network analysis of a large opiate-driven outbreak of HIV infection in the United States. J Infect Dis 216(9):1053–62
2. Qiao YC, Xu Y, Jiang DX, Wang X, Wang F, Yang J, Wei YS (2019) Epidemiological analyses of regional and age differences of HIV/AIDS prevalence in China, 2004–2016. Int J Infect Dis 81:215–20
3. Paraskevis D, Nikolopoulos G, Tsiara C, Paraskeva D, Antoniadou A, Lazanas M, Hatzakis A (2011) HIV-1 outbreak among injecting drug users in Greece, 2011: a preliminary report. Eurosurveillance 16(36):19962

4. Doitsh G, Greene WC (2016) Dissecting how CD4 T cells are lost during HIV infection. Cell Host Microbe 19(3):280–91
5. Cummins NW, Badley AD (2014) Making sense of how HIV kills infected CD4 T cells: implications for HIV cure. Mol Cell Ther 2(1):20
6. Poorolajal J, Hooshmand E, Mahjub H, Esmailnasab N, Jenabi E (2016) Survival rate of AIDS disease and mortality in HIV-infected patients: a meta-analysis. Public Health 139:3–12
7. Alemu A, Yesuf A, Zerihun B, Getu M, Worku T, Bitew ZW (2020) Incidence and determinants of tuberculosis among HIV positives in Addis Ababa, Ethiopia: a Retrospective Cohort Study. Int J Infect Dis 95:59
8. WHO (2018) Global Tuberculosis Report Geneva
9. Ramírez BC, Vega YC, Shepherd BE, Le C, Turner M, Frola C, McGowan CC (2017) Outcomes of HIV-positive patients with cryptococcal meningitis in the Americas. Int J Infect Dis 63:57–63
10. Rajasingham R, Smith RM, Park BJ, Jarvis JN, Govender NP, Chiller TM, Boulware DR (2017) Global burden of disease of HIV-associated cryptococcal meningitis: an updated analysis. Lancet Infect Dis 17(8):873–81
11. Mekonnen Y, Hadush T, Tafere A, Tilahun A (2016) A review article on cryptosporidiosis
12. Sullivan MC, Rosen AO, Allen A, Benbella D, Camacho G, Cortopassi AC, Kalichman SC (2020) Falling Short of the First 90: HIV Stigma and HIV Testing Research in the 90-90-90 Era
13. Li D, Ma W (2007) Asymptotic properties of a HIV-1 infection model with time delay. J Math Anal Appl 335:683–91
14. Abdullahi YM, Nweze O (2011) A simulation of an sir mathematical model of HIV transmission dynamics using the classical Euler's method. Shiraz Med J 12:196–202
15. Jiang X, Chen X, Huang T, Yan H (2021) Bifurcation and control for a predator-prey system with two delays. IEEE Trans Circuits Syst II Express Briefs 68(1):376–80
16. Jiang X, Chen X, Chi M, Chen J (2020) On Hopf bifurcation and control for a delay systems. Appl Math Comput 370(1):124906
17. Asif M, Ullah Jan S, Haider N, Mdallal QA, Jawad TA (2020) Numerical modeling of NPZ and SIR models with and without diffusion. Result Phys 19:103512
18. Asif M, Khan ZA, Haider N, Mdallal QA (2020) Numerical simulation for solution of SEIR models by meshless and finite difference methods. Chaos Soliton Fractals 141:110340
19. Hajji MA, Mdallal QA (2018) Numerical simulations of a delay model for immune system tumor interaction. Sultan Qaboos Univ J Sci 23(1):19–31
20. Rihan FA, Al-Mdallal QM, AlSakaji HJ, Hashish A (2019) A fractional-order epidemic model with time-delay and nonlinear incidence rate. Chaos Solitons Fractals 126:97–105
21. Ullah I, Ahmad S, Mdallal QA, Khan ZA, Khan H, Khan A (2020) Stability analysis of a dynamical model of tuberculosis with incomplete treatment. Adv Differ Equ. https://doi.org/10.1186/s13662-020-02950-0
22. Kumar S, Chauhan RP, Abdel-Aty AH, Alharthi MR (2021) A study on transmission dynamics of HIV/AIDS model through fractional operators. Results Phys 22:103855
23. Yu P, Zhang W (2019) Complex dynamics in a unified SIR and HIV disease model: a bifurcation theory approach. J Nonlinear Sci 29(5):2447
24. Dhar M, Bhattacharya P (2019) Analysis of SIR epidemic model with different basic reproduction numbers and validation with HIV and TSWV data, Iran. J Sci Technol Trans A Sci 43(5):2385
25. Naik PA, Zu J, Owolabi KM (2020) Global dynamics of a fractional order model for the transmission of HIV epidemic with optimal control. Chaos, Solitons Fractals 138:109826
26. Wang X, Wang W, Li Y (2021) Global stability of switched HIV/AIDS models with drug treatment involving caputo-fractional derivatives. Discret Dyn Nat Soc 138:109826
27. Babaei A, Jafari H, Liya A (2020) Mathematical models of HIV/AIDS and drug addiction in prisons. Eur Phys J Plus 135(5):1
28. Chang H (2021) A mathematical study on the drug resistant virus emergence with HIV/AIDS treatment cases. Heliyon 7(1):e05883
29. Bassey BE, Henry AO (2021) Global stability analysis of the role of antiretroviral therapy (ART) abuse in HIV/AIDS treatment dynamics. Pure Appl Math J 10(1):9
30. Wanduku (2020) A nonlinear multi-population behavioral model to assess the roles of education campaigns, random supply of aids, and delayed ART treatment in HIV/AIDS epidemics. Math Biosci Eng 17(6):6791
31. Teklu SW, Mekonnen TT (2021) HIV/AIDS-pneumonia coinfection model with treatment at each infection stage: mathematical analysis and numerical simulation. J Appl Math 2021:1–21
32. Kumar S, Chauhan RP, Momani S, Hadid S (2020) Numerical investigations on COVID-19 model through singular and non-singular fractional operators. Numer Methods Partial Differ Equ. https://doi.org/10.1002/num.22707
33. Khan MA, Ullah S, Kumar S (2021) A robust study on 2019-nCOV outbreaks through non-singular derivative. Eur Phys J Plus. https://doi.org/10.1140/epjp/s13360-021-01159-8
34. Kumar S, Kumar A, Samet B, Dutta H (2020) A study on fractional host-parasitoid population dynamical model to describe insect species. Numer Methods Partial Differ Equ 37:1673–1692
35. Mohammadi H, Kumar S, Rezapour S, Etemad S (2021) A theoretical study of the Caputo-Fabrizio fractional modeling for hearing loss due to Mumps virus with optimal control. Chaos, Solitons Fractals 144:110668
36. Kumar S, Kumar R, Cattani C, Samet B (2020) Chaotic behaviour of fractional predator-prey dynamical system. Chaos, Solitons Fractals 135:109811
37. Kumar S, Kumar R, Osman MS, Samet B (2021) A wavelet based numerical scheme for fractional order SEIR epidemic of measles by using Genocchi polynomials. Numer Methods Partial Differ Equ 37:1250–1268
38. Ammi MRS, Tahiri M, Tilioua M, Zeb A, Khan I, Andualem M (2022) Global analysis of a time fractional order spatio-temporal SIR model. Sci Rep 12:5751
39. Fraser C, Donnelly CA, Cauchemez S et al (2009) Pandemic potential of a strain of influenza A (H1N1): early findings. Science 324:1557–1561
40. Chakrabrty A, Singh M, Lucy B, Ridland P (2007) Predator-prey model with pry-taxis and diffusion. Math Comput Model 46:482–98
41. Ahmed N, Tahira SS, Rafiq M, Rehman MA, Ali M, Ahmad MO (2019) Positivity preserving operator splitting nonstandard finite difference methods for SEIR reaction diffusion model. Open Math 17:313–30
42. Lin Z, Pederson M (2004) Stability in a di usive food-chain model with Michaelis-Menten functional response. Nonlinear Anal 57:421–433
43. Ahmed N, Rafiq M, Rehman MA, Iqbal MS, Ali M (2019) Numerical modeling of three dimensional Brusselator system. AIP Adv 09(01):01–19
44. Charpentier BMC, Kojouharov HV (2013) Unconditionally positive preserving scheme for advection-diffusion-reaction equations. Math Comput Model 57(10):2177–1285
45. Fujimoto T, Ranade R (2004) Two characterizations of inverse positive matrices: the Hawkins-Simon condition and the le chatelier-braun principle. Electron J Linear Algebra ELA 11(1):01–18
46. Smith GD (1985) Numerical solution of partial differential equations: finite difference methods, 3rd edn. Clarendon Press, Oxford
47. Mitchell AR, Griffiths DF (1980) Finite difference methods in partial differential equations. T. Wiley, Hoboken

48. Chinviriyasit S, Chinviriyasit W (2010) Numerical modelling of an SIR epidemic model with diffusion. Appl Math Comput 216:395–409
49. Kustiawan C (2018) A Numerical scheme for a reaction diffusion equation with time delay and impulses. Far East J Math Sci 106(2):451–62
50. Ahmed N, Elsonbaty A, Adel W, Baleanu D, Rafiq M (2020) Stability analysis and numerical simulations of spatiotemporal HIV CD4+ T cell model with drug therapy. Chaos 30:083122
51. Samsuzzoha M, Singh M, Lucy D (2013) Parameter estimation of influenza epidemic model. Appl Math Comput 220:616
52. Kristensen MR (2014) Parameter estimation in nonlinear dynamical systems Master's Thesis. Technical University of Denmark, Kongens